

1

2 **Anthropogenic VOC in Abidjan, southern West Africa: from source** 3 **quantification to atmospheric impacts**

4

5 Pamela Dominutti^{1*}, Sekou Keita ^{2,3}, Julien Bahino^{2,3}, Aurélie Colomb¹, Cathy Liousse², Veronique
6 Yoboué³, Corinne Galy-Lacaux², Eleanor Morris⁴, Laëtitia Bouvier¹, Stéphane Sauvage⁵ and Agnès
7 Borbon¹

8

9 ¹ Université Clermont Auvergne, CNRS, Laboratoire de Météorologie Physique (LaMP), F-63000 Clermont-Ferrand,
10 France.

11 ² Laboratoire d'Aérodologie, Université Paul Sabatier Toulouse 3 - CNRS, Toulouse, France

12 ³ Laboratoire de Physique de l'Atmosphère (LAPA)- Université Felix Houphouët-Boigny, Abidjan, Côte d'Ivoire

13 ⁴ Wolfson Atmospheric Chemistry Laboratories, Department of Chemistry, University of York, Heslington, York,
14 YO10 5DD, UK

15 ⁵ IMT Lille Douai, Sciences de l'Atmosphère et Génie de l'Environnement (SAGE), Douai, France

16 **Now at Wolfson Atmospheric Chemistry Laboratories, Department of Chemistry, University of York, Heslington,*
17 *York, YO10 5DD, UK*

18

19 Correspondence to P. Dominutti (pamela.dominutti@york.ac.uk) + A. Borbon (agnes.borbon@uca.fr)

20

21 **Abstract**

22 Several field campaigns were conducted in the framework of the Dynamics-Aerosol-Chemistry-Cloud Interactions
23 in West Africa (DACCIWA) project to measure a broad range of atmospheric constituents. Here we present the
24 analysis of an unprecedented and comprehensive dataset integrating up to fifty-six volatile organic compounds
25 (VOCs) from ambient sites and emission sources. VOCs were collected on [multisorbent tubes](#) in the coastal city of
26 Abidjan, Côte d'Ivoire, in winter and summer 2016 and later analysed by gas chromatography coupled with flame
27 ionization and mass spectrometer detectors (GC-FID and GC-MS) [at the laboratory](#).

28 The comparison between VOC emission source profiles and ambient profiles suggests the substantial impact of two-
29 stroke motorized two-wheel vehicles and domestic fires on the composition of Abidjan's atmosphere. However,
30 despite high VOC concentrations near-source, moderate ambient levels were observed (by a factor of 10 to 4000
31 lower), similar to the concentrations observed in northern mid-latitude urban areas. Besides photochemistry, the
32 reported high wind speeds seem to be an essential factor that regulates air pollution levels in Abidjan.

33 Emission ratios ($\Delta\text{VOC}/\Delta\text{CO}$) were established based on real-world measurements achieved for a selected number
34 of representative combustion sources. Maximum measured molar mass emissions were observed from two-wheel
35 vehicles (TW), surpassing other regional sources by two orders of magnitude. Local practices like waste burning also
36 make a significant contribution to VOC emissions, higher than those from light-duty vehicles by 1.5 to 8 orders of
37 magnitude. These sources also largely govern the VOC's atmospheric impacts in terms of OH reactivity, secondary

38 organic aerosol formation (SOAP) and photochemical ozone creation potential (POCP). While the contribution of
39 aromatics dominates the atmospheric impact, our measurements reveal the systematic presence of anthropogenic
40 terpenoids in all residential combustion sectors. Finally, emission factors were used to retrieve and quantify VOC
41 emissions from the main anthropogenic source sectors at the national level. Our detailed estimation of VOC emissions
42 suggests that the road transport sector is the dominant source in Côte d'Ivoire, emitting around 1200 Gg yr⁻¹ of gas-
43 phase VOCs. These new estimates are 100 and 160 times larger than global inventory estimations from MACCity or
44 EDGAR (v4.3.2), respectively. Additionally, the residential sector is largely underestimated in the global emission
45 inventories, by a factor of 13 to 43. Considering only Côte d'Ivoire, these new estimates for VOCs are three to six
46 times higher than the whole of Europe. Given the significant underestimation of VOC emissions from transport and
47 residential sectors in Côte d'Ivoire, there is an urgent need to build more realistic and region-specific emission
48 inventories for the entire West African region. This might be not only true for VOCs but for all atmospheric
49 pollutants. The lack of waste burning, wood fuel burning and charcoal burning and fabrication representation in
50 regional inventories also needs to be addressed, particularly in low-income areas where these types of activities are
51 ubiquitous sources of VOC emissions.

52

53 **Keywords: VOCs, emission inventories, West Africa, air pollution, emission ratios.**

54

55 1. Introduction

56 The West Africa region, located to the north of the Gulf of Guinea, is one of the most populated areas in Africa with
57 more than 300 million inhabitants in 2016 (United Nations, 2017). The population has increased by a factor of five
58 since 1950, making West Africa the fastest growing region in the world. Furthermore, future projections indicate
59 population densities in developing countries will continue to increase. The impact in Africa will be particularly high,
60 with projections indicating that the population of the continent could represent 40% of the world's population by
61 2100 (United Nations, 2017). The unplanned explosive growth of urban centres in the region is a significant issue,
62 with water access, air pollution, health problems and unregulated emissions being identified as major concerns.

63 These emissions can produce diverse effects on atmospheric chemistry which are enhanced by severe photochemical
64 conditions and dynamic atmospheric interactions. The atmospheric composition over West Africa is affected by air
65 masses transported from remote sources, i.e., aerosol dust from the Sahara Desert, biomass burning plumes and local
66 urban pollution (Knippertz et al., 2017; Mari et al., 2011). Observations performed during the AMMA (African
67 Monsoon Multidisciplinary Analysis, West Africa, 2005-2006) campaign showed that air quality issues are
68 predominantly related to traffic and combustion emissions (Mari et al., 2011). Residential emissions in Southern
69 West Africa (SWA) are attributed to charcoal and wood burning as they are primary sources of domestic energy,
70 widely used for cooking and heating activities. Regional biomass burning is a significant source of carbonaceous
71 aerosols and volatile organic compounds (VOCs) that can have effects on public health and climate through the
72 formation of secondary pollutants (Gilman et al., 2015; Knippertz et al., 2015b; Sommers et al., 2014).

73 Additionally, in most of the SWA cities, traffic emissions are major sources of air pollution (Assamoi and Liousse,
74 2010). The road transport sector is largely disorganized due to the underdevelopment of road networks and to the
75 absence of a regulation policy for public transportation (Assamoi and Liousse, 2010). As a result, TW vehicles are

76 widely used in the cities for short-distance travel, replacing public transport. Furthermore, the vehicle fleet has
77 increased in the last year, which is characterized in most cities by a large number of old vehicles (Keita et al., 2018).
78 Over the next few years, African emissions from the combustion of fossil fuels, biofuels, and refuse are expected to
79 increase considerably and could represent about 50% of the global emissions of organic carbon (Knippertz et al.,
80 2017; Liousse et al., 2014). However, emission estimates are uncertain and detailed emission inventories are still
81 required for a better estimation of their impacts on climate change and health over this highly sensitive region
82 (Knippertz et al., 2017).

83 VOCs include a large number of species which can affect air quality by producing secondary pollutants such as ozone
84 and secondary organic aerosols (Seinfeld and Pandis, 2006). Given the reactive nature of VOCs (Atkinson and Arey,
85 2003), VOC emissions need to be disaggregated by species or species groups for a better representation of their
86 chemical features, and to assess their impacts on the secondary formation processes. As VOCs are significant
87 pollutants present in urban atmospheres, in-situ VOC observations are necessary to directly assess exposure and to
88 improve the prediction of secondary product formation.

89 Several field campaigns have been conducted in the last twenty years all over the world with the purpose of
90 characterizing VOC species to better understand their emission sources and fate (Bechara et al., 2010; Bon et al.,
91 2011; Borbon et al., 2013; Brito et al., 2015; Dominutti et al., 2016; Kumar et al., 2018; Salameh et al., 2015; Wang
92 et al., 2014; Warneke et al., 2007). In particular, VOC field observations have been intensely used as constraints for
93 the development of reliable emission inventories (Borbon et al., 2013; Boynard et al., 2014; Gaimoz et al., 2011;
94 Niedojadlo et al., 2007; Salameh et al., 2016b). Some of these studies pointed out significant discrepancies between
95 inventory estimations and emission ratios derived from ambient measurements, implying some limitations in the
96 accurate modelling of VOCs impacts. For northern mid-latitude cities, discrepancies up to a factor of 10 for VOC
97 emissions have been observed (Borbon et al., 2013; Boynard et al., 2014). Such discrepancies are expected to be even
98 more substantial in places of the developing world with high anthropogenic pressures like Africa and South America
99 (Huang et al., 2017). For Africa in particular, the emission inventories frequently used are those developed for global
100 scales due to the lack of observations, which involve numerous uncertainties (Keita et al., 2018; Liousse et al., 2014).
101 While global emission inventories commonly estimate the total mass of speciated VOCs, they fail in reproducing the
102 spatial and temporal variability of VOC emission speciation. Indeed, the emission composition can change depending
103 on the emission source, fuel quality, combustion technologies, and main regional practices (Huang et al., 2017). The
104 use of activity data and emission factors derived from local measurements of regional-specific sources may help to
105 reduce the uncertainties in those emission inventories. In a recent study calculated the emission factors (EFs) of
106 different compounds and activities in SWA (Keita et al., 2018). A comparison of the emissions calculated from the
107 EFs with those observed from the EDGARv4.3.2 (Huang et al., 2017) inventory showed a marked discrepancy (factor
108 of 50 difference) for fifteen VOCs species (3 alkanes, 8 aromatics, isoprene and 3 monoterpenes) in Côte d'Ivoire.
109 That study emphasised the importance of considering African anthropogenic emissions at regional scales. Due to the
110 scarcity of suitable data, the uncertainties in the observations cannot currently be assessed and more detailed studies
111 are required to quantify these uncertainties. Characterization and quantification of the emissions is crucial for
112 improving our understanding of the contributions of anthropogenic and natural sources to the atmospheric
113 composition over SWA, and for assessing their impact on public health and air quality conditions.

114 Several intensive field campaigns in the framework of the Dynamics-Aerosol-Chemistry-Cloud-Interactions in West
115 Africa (DACCIWA) project were conducted in 2015 and 2016 (Knippertz et al., 2015a). Here, we present the results
116 obtained from the VOC field campaigns at different sites, including ambient and near-source measurements, in one
117 of the major SWA cities: Abidjan in Côte d'Ivoire. Abidjan is the economic capital of Côte d'Ivoire with a population
118 of 6.5 million (in 2016), representing more than 20 % of the population of the country (United Nations, 2017). Along
119 with autonomous districts, Abidjan encompasses an area of 2119 km² and is distinguished by remarkable
120 industrialization and urbanization. In summer, West Africa is influenced by monsoon phenomenon which is mainly
121 driven by the surface pressure contrast between the relatively cold waters of the tropical Atlantic Ocean and the
122 Saharan heat low (Knippertz et al., 2017). This seasonal circulation characterized the wet (summer) and dry (winter)
123 periods in the region. During the dry season (November to February), most of the region is dominated by dry
124 northeasterly winds from the Sahara and the precipitation is confined to the coast, where the sea-breeze circulation
125 provides humid air and produces near-surface convergence. Then, the monsoon starts its development and
126 southwesterly moist winds begin to enter deeper into the continent producing more clouds and precipitation between
127 July and August. The strong pressure and temperature gradients between the Atlantic Ocean and the Sahara drive the
128 strong monsoon flow northward along with southwesterlies, reaching higher latitudes up to 20° N (Knippertz et al.,
129 2015b).

130 Speciated VOCs were collected during DACCIWA using sorbent tubes, and then analysed and quantified at the
131 laboratory applying different gas chromatography techniques. These data provide the first constraints for the
132 construction of a regional emission inventory and for understanding the role of anthropogenic VOC emissions in
133 regional atmospheric chemistry.

134 This work aims to establish and analyse the spatial distribution of VOC concentrations and VOC speciated profiles
135 of primary anthropogenic sources in Abidjan by performing sampling under real-conditions. These sources include
136 traditional and regional-specific ones, such as road transportation (gasoline and diesel emissions from different
137 vehicles), charcoal fabrication, and burning emissions from domestic cooking fires, landfill waste, and hardwood
138 fuel. This new dataset provides substantial information enabling the quantification of VOC emissions for several
139 sources in Côte d'Ivoire. These source profiles are analysed and contrasted with those provided by global emission
140 inventories. Finally, the impact on air quality due to the use of regional-specific sources is assessed in terms of
141 reactivity and secondary pollutant formation.

142

143 **2. Materials and Methods**

144 As part of the DACCIWA project, intensive field campaigns were performed in 2015 and 2016, focusing for the first
145 time on the most populated southern coastal region of West Africa. The DACCIWA campaign had an emphasis on
146 atmospheric composition, including air pollution, health impacts and cloud-aerosol interactions (Knippertz et al.,
147 2015a). Here we present new results from intensive ambient measurements in Abidjan and an extended VOC
148 speciation from source emission measurements. These results are part of the activities developed under the
149 workpackage 2 (WP2) - Air Pollution and Health - which aims to link and quantify emission sources, air pollution
150 and related health impacts over different urban sources in West Africa (Knippertz et al., 2015a).

151

152

154 2.1 Sampling

155 The field campaigns were conducted in Abidjan, Côte d'Ivoire during summer and winter according to the strategic
156 directions of the DACCIWA WP2. Two types of cartridges were deployed for VOC measurements: single sorbent
157 cartridge made of Tenax TA 60-80 mesh (250 mg) or multi-sorbent cartridges made of Carbopack B (200mg) and
158 Carbopack C (200 mg (carbotrap 202) purchased from Perkin Elmer). The combination of different sorbent materials
159 allowed the sampling of 10 aromatics (C₆-C₉), 22 n-alkanes (C₅-C₁₆), 10 monoterpenes, 7 aldehydes, isoprene, and
160 other oxygenated compounds. All compounds are reported in Table S1. Before the sampling, cartridges were
161 conditioned by flowing purified nitrogen, at a rate of 100 mL min⁻¹ for 5 hours at 320°C.

162 Firstly, ambient VOC were collected to analyse their spatial distribution in Abidjan. Ambient measurements were
163 performed at nine sites, which are shown in Figure 1. The distribution of the sampling locations was selected
164 according to the primary source locations. They include urban background sites and areas impacted by residential,
165 road transport, domestic fires, waste burning and industrial activities. The characteristics and geographical location
166 of each site are reported in Table 2. The ambient campaigns were conducted during the dry season (February 2016).
167 Samples were collected every 2 days at different times of the day (from 6 a.m. to 8 p.m.) by using a manual pump
168 (Accuro 2000, Dräger) at 100 sccm (standard cubic centimetres per minute) flow rate. One single sorbent tube was
169 exposed six times at each sampling location. In total, 3.6 L of air were collected at each site for a single 600 mL
170 volume each time. [Details on the sampling strategy are reported in Table S3.](#)

171 Secondly, direct source emission measurements were performed to obtain VOC emission profiles from the main
172 anthropogenic sources in Abidjan. The sources include traditional ones like road transportation, and SWA regional
173 specific ones such as domestic waste burning, charcoal fabrication, charcoal burning as well as wood fuel burning
174 (Table 1). Despite that part of these measurements for a limited number of VOC (fifteen species including 3 alkanes,
175 8 aromatics, 3 terpenes and isoprene) and particles were discussed somewhere (Keita et al., 2018), we improve the
176 VOC database extended to 56 VOC species measured in the follow source emissions:

- 177 - For road transportation, analysis of different vehicle exhaust measurements was carried out. Samples
178 integrate five road transportation sub-categories: heavy-duty diesel vehicles (HDDV, trucks, and buses – 3
179 samples on Tenax and 3 samples on Carbopack tubes), light-duty diesel vehicles (LDDV, diesel cars, 2
180 samples on Tenax tubes), light-duty gasoline vehicles (LDGV, gasoline cars, 2 samples on Tenax tubes),
181 two-wheel two-stroke (TW 2T, 3 samples on Tenax and 3 samples on Carbopack tubes) and two-wheel four-
182 stroke (TW 4T, 3 samples on Tenax and 3 samples on Carbopack tubes) vehicles. Differences in fuel type
183 (gasoline and diesel) and the fleet age have been considered. In African countries, two-wheeled vehicles
184 (two-stroke or four-stroke engines) frequently use a mixture of oil and gasoline derived from smuggling,
185 which is characterized by high pollutant emissions (Assamoi and Liousse, 2010).
- 186 - Regarding domestic waste-burning (WB), samples were obtained (5 samples on Tenax tubes) at the official
187 domestic landfill site located to the east of Abidjan (AD, Figure 1 and Table 2). The sampling was performed
188 inside the waste burning plume to integrate the different combustion processes involved.
- 189 - Charcoal-burning (CH) and wood fuel burning (FW) are common cooking and heating practices in African
190 urban areas. FW emissions were obtained by measuring the fire plume of tropical African hardwood,
191 specifically Hevea (*Hevea brasiliensis*). FW and CH were burned in two types of stoves traditionally used

192 in the SWA region for cooking, which are made of metal and baked earth. The measurements included all
193 the combustion phases (Keita et al., 2018) (4 samples on Tenax and 3 samples on Carbopack tubes).
194 – The charcoal-making (CHM) profile was obtained by measuring emissions from traditional kilns, that use
195 different types of dense wood. The kiln was covered with a layer of leaves and another one of soil of about
196 10 cm thickness. The smoke was sampled through holes made in the CHM kiln, which are located in the
197 horizontal plane, and provide the air circulation for the pyrolysis propagation (Keita et al., 2018) (2 samples
198 one on Tenax and one on Carbopack tubes).

199 All samples were obtained in the emission plume at around 1–1.5m from the source, except for vehicles where
200 samples were taken at the tailpipe outlet while the vehicle's engine was idling. Carbon monoxide (CO) and carbon
201 dioxide (CO₂) measurements were also performed on the emission sources together with the VOC measurements.
202 For this, the QTRAK-7575 sensor (TSI, Keita et al., 2018) was used to measure real-time CO₂ and CO gas
203 concentrations. CO is measured by using an electrochemical sensor with a sensitivity of 0 to 500 ppm with ±3%
204 accuracy. CO₂ concentrations are obtained by using a non-dispersive infrared detector with a sensitivity of 0 to 5000
205 ppm with an accuracy of ±3 %. The instrument was calibrated in the laboratory prior to each emission measurement
206 These concentrations were used for the estimation of EF values from different samples, which were later averaged
207 for every source category. [Details on the sampling strategy at emission are reported in Table S4.](#)

208

209 2.2 Analytical instrumentation

210 Duplicate measurements were performed and analysed in two different laboratories to investigate the reproducibility
211 of analytical techniques and to acquire a wider range of VOC species. The analysis of the Tenax TA tubes was
212 performed at the *Laboratoire de Météorologie Physique* (LaMP, Clermont-Ferrand, France) using a gas
213 chromatograph mass spectrometer system (GC/MS, Turbomass Clarus 600, Perkin Elmer®) coupled to automatic
214 thermal desorption (Turbomatrix ATD). Each tube was desorbed at 270°C for 15 min at a flow rate of 40 mL min⁻¹
215 and pre-concentrated on a second trap, at -30°C containing Tenax TA. After the cryofocusing, the trap was rapidly
216 heated to 300°C (40° s⁻¹) and the target compounds were flushed into the GC. Due to the high loads in some samples,
217 an inlet and outlet split of 5 mL min⁻¹ and 2 mL min⁻¹ were set up, respectively. The analytical column was a PE-
218 5MS (5% phenyl – 95% PDMS, 60m×0.25mm×0.25µm) capillary column (Perkin Elmer) and a temperature ramp
219 was applied to guarantee the VOCs separation (35°C for 5 minutes, heating at 8°C min⁻¹ to 250°C, hold for 2
220 minutes). The mass spectrometer was operated in a Total Ion Current (TIC) from 35 to 350 m/z amu. Chromatography
221 parameters were optimized to enable good separation of fifteen identified compounds by a complete run of 34
222 minutes on each cartridge. Calibration was performed by analysing conditioned cartridges doped with known masses
223 of each compound, present in certified standard low-ppb gaseous standard, purchased from the National Physical
224 Laboratory (NPL, UK; 4 ppb ±0.8 ppb). That method provided the separation and identification of 16 compounds,
225 from C₅ to C₁₀ VOCs, including 8 aromatics, 3 monoterpenes, 4 alkanes and isoprene. [The limit of detection lies
226 between 1.10 ppt \(1,2,3-trimethylbenzene\) and 22.6 ppt \(2-methylpentane\). The global uncertainty is estimated
227 between 5% and 38%.](#)

228 Carbopack tubes analysis was carried out by applying a gas chromatography-flame ionization detector (ATD-GC-
229 FID, Perkin Elmer) system at the *SAGE Department (IMT Lille Douai)*. The cartridges were previously thermo-
230 desorbed at 350°C for 15 minutes with a helium flow of 20 mL min⁻¹. This method allowed the separation and

231 identification of up to 56 compounds, from C₅–C₁₆ VOCs, including 7 aldehydes, 4 ketones, 10 monoterpenes and 6
232 long-chain alkanes from C₁₂ to C₁₆. More details on the analytical technique can be found elsewhere (Ait-Helal et
233 al., 2014; Detournay et al., 2011). VOCs can be classified according to their saturation concentration, C*, which
234 indicates their volatility (Ait-Helal et al., 2014; Epstein et al., 2010; Robinson et al., 2007). Here, C₁₂–C₁₆ alkanes
235 are classified as VOC of intermediate volatility, since given their C* values are between 10³ μg m⁻³ <C* < 10⁶ μg m⁻³
236 (Ait-Helal et al., 2014). The detection limits lie between 1 ppt to 13 ppt (hexadecanal) and the global uncertainty
237 varies between 3.7% and 32.6% as detailed elsewhere (Detournay et al., 2011; Keita et al., 2018).

238 The application of both methods allowed the comparison of common compounds that were measured at ambient sites
239 and sources (benzene, toluene, ethylbenzene, m+p-xylene, o-xylene, trimethylbenzenes, n-heptane, iso-octane, n-
240 octane, α-pinene, β-pinene, limonene, isoprene) and the performance analysis of the analytical techniques.
241 Furthermore, the combination of different sorbent tubes and analytical strategies allowed the quantification of a
242 higher number of VOC species, and therefore, a more extensive analysis of source contributions.

243

244 2.3 Metrics and calculations

245 Different calculations were implemented to assess the VOC emissions and their impacts in Abidjan. Here we provide
246 the mathematical basis for each investigated parameter. Firstly, the emission factors (EF) were computed for the
247 whole extended VOC database (56 compounds) following the methodology described in Keita et al. (2018). EFs
248 combined with regional statistics were later used for the estimation of VOC emissions in Côte d'Ivoire for each
249 source category. Secondly, the emission ratios (ER) of each VOC species related to CO for all the emission sources
250 were established. Finally, the reported ERs were used to evaluate the impacts on atmospheric reactivity by applying
251 commonly used metrics.

252

253 2.3.1 Emission factors and quantification of VOC emissions

254 VOC emission factors were estimated from the concentrations measured for all the emission sources, as follows

$$255 \quad EF(VOC) = \frac{\frac{\Delta VOC}{\Delta CO + \Delta CO_2} \times MW_{VOC}}{12} \times fc \times 10^3 \quad (1)$$

256 where EF (VOC) is the emission factor of the specific VOC in gram per kilogram of burned fuel (g kg⁻¹); ΔVOC =
257 [VOC]_{emission} – [VOC]_{background} is the VOC mixing ratio in the emission and background air respectively, in parts per
258 billion by volume (ppbv), MW_{VOC} is the molar weight of the specific VOC (in g mol⁻¹), 12 is the molar weight of
259 carbon (g mol⁻¹) and *fc* is the mass fraction of carbon in the fuel analysed. The *fc* values used were obtained from the
260 literature and applied to each source. The EF for selected fifteen VOCs were already published and more details
261 about the method can be found elsewhere (Keita et al., 2018). Here we applied the same method for the whole VOC
262 database, including 56 compounds directly measured from the emission sources. For this, VOC emissions were
263 estimated using the emission factors obtained from near-source measurements along with the statistical International
264 Energy Agency (IEA) activity data, available for the different sources). Equation 1 was used to compute the emission
265 factors, considering all the VOC species measured and including the mass fraction of each fuel (*fc*) obtained from
266 the literature. Additionally, the differences in fuel type and the fleet age have been considered, as well as the fleet
267 distribution by calculating the equivalent vehicular fleet. For the road transport sector, the equivalent fleet means
268 were calculated considering the fleet characteristics in Côte d'Ivoire, as detailed in Keita et al. (2018). These

269 calculations were based on the information given by the Direction Generale des Transports Terrestres in Côte
270 d'Ivoire, which considered that 60% of vehicles are old models and 77% of the total fleet is composed by light-duty
271 vehicles. Regarding TW, 60% of them are two-stroke engines and only 40% of the total are considered as recent
272 vehicles (SIE CI, 2010). In the residential profile, we integrated the emissions measured from CH, CHM and FW
273 sources, commonly observed at residential sites in Abidjan. Afterwards, the mean road transportation and residential
274 profiles for Côte d'Ivoire were computed and compared with two referenced global inventories, EDGAR v4.3.2 and
275 MACCity (Granier et al., 2011; Huang et al., 2017).

276

277 2.3.2 Molar mass emission ratios

278 Emission ratios (ER) were obtained by dividing each VOC mixing ratio by carbon monoxide (CO) mixing ratios as
279 follows:

$$280 \quad ER = \frac{[\Delta VOC] \text{ ppbv}}{[\Delta CO] \text{ ppmv}} \quad (2)$$

281 We selected CO as a combustion tracer because most VOCs and CO are co-emitted by the target sources.
282 Furthermore, ratios to CO are regularly reported in the literature for biomass burning and urban emissions (Baker et
283 al., 2008; Borbon et al., 2013; Brito et al., 2015; Gilman et al., 2015; de Gouw et al., 2017; Koss et al., 2018; Wang
284 et al., 2014) which are useful constraints for further comparisons. Emission ratios were calculated in ppbv of VOC
285 per parts per million by volume (ppmv) of CO, which is similar to a molar ratio (mmol VOC per mol CO). Molar
286 mass (MM) emission ratios were also computed following Gilman et al. (2015). MM is the VOC mass emitted (μg
287 m^{-3}) per ppmv CO, obtained from equation 2 and converted by using the VOC molecular weight (MW) (g mol^{-1})
288 and the molar volume (24.86 L at 1 atm and 30°C). Table S1 includes the emission ratios obtained for each VOC and
289 MW values used.

290

291 2.3.3 VOC-OH reactivity

292 The OH reactivity was estimated to evaluate the potential contribution of each measured VOC to the photochemical
293 processing. VOC-OH reactivity represents the sink reaction of each VOC with the hydroxyl radical (OH) and is equal
294 to

295

$$296 \quad VOC_{OH \text{ reactivity}} = ER \times k_{OH} \times CF, \quad (3)$$

297 where ER is the emission ratio for each VOC related to CO (ppbv per ppmv), k_{OH} is the second-order reaction rate
298 coefficient of VOC with the hydroxyl radical ($\times 10^{-12} \text{ cm}^3 \text{ molecule}^{-1} \text{ s}^{-1}$) and CF is the conversion factor of molar
299 concentration ($2.46 \times 10^{10} \text{ molecule cm}^{-3} \text{ ppbv}^{-1}$ at 1 atm and 25°C) (Gilman et al., 2015). k_{OH} values for all VOC
300 species were obtained from Atkinson and Arey (2003) and the NIST Chemical Kinetics Database (Manion et al.,
301 2015).

302

303 2.3.4 Ozone Formation Potential

304 The oxidation of VOCs is often initiated by the reaction with the hydroxyl radical ($\cdot\text{OH}$), which in the presence of
305 NO_x ($\text{NO} + \text{NO}_2$) leads to the photochemical formation of O_3 . The ozone formation potential represents the ability of
306 each VOC to produce tropospheric ozone and it was calculated as follows:

307

308
$$VOC_ozone\ formation\ potential = ER \times POCP, \quad (4)$$

309 where the ER is the emission ratio of each VOC related to CO (ppbv of VOC per ppmv of CO) and POCP is the
310 photochemical ozone creation potentials developed in previous studies (Derwent et al., 2007; Jenkin et al., 2017).
311 POCP values were obtained by simulating a realistic urban mass trajectory with the Master Chemical Mechanism
312 (MCM). This model estimates the change in ozone production by incrementing the mass emission of each VOC
313 (Derwent et al., 1998). POCPs for an individual VOC are estimated by quantifying the effect of a small increase in
314 its emission on the concentration of the formed modelled ozone, respective to that resulting from the same increase
315 in the ethene emission (POCP value for ethene is, therefore, 100). In this study, POCP values were analysed on VOC
316 family basis obtained from a recent study (Huang et al., 2017), or adapted from individual POCP values.

317

318 2.3.5 Secondary organic aerosol (SOA) formation potential

319 The SOA formation potential represents the propensity of each VOC to form secondary organic aerosols and is equal
320 to

321
$$SOA_VOC\ formation\ potential = ER \times SOAP, \quad (5)$$

322 where ER is the emission ratio for each measured VOC related to CO (ppbv of VOC per ppmv of CO) and SOAP is
323 a non-dimensional model-derived SOA formation potential (Derwent et al., 2010; Gilman et al., 2015). All SOAP
324 values represent the modelled mass of organic aerosol that were formed per mass of VOC reacted on an equal mass
325 emitted basis relative to toluene. Toluene was selected as the reference compound due to its well-known emissions
326 and it is usually documented as a critical anthropogenic SOA precursor (Derwent et al., 2010).

327

328 ER, k_{OH} and SOAP values for each VOC and each source are detailed in Table S1. In the absence of SOAP values
329 for specific compounds, we estimated the values (indicated in Table S1, referred as ^a) by using those of comparable
330 compounds based on similar chemical properties, as suggested in the study of Gilman et al. (2015).

331

332 2.4 Ancillary data

333 Meteorological observations were provided by the NOAA Integrated Surface Database (ISD; <https://www.ncdc.noaa.gov/isd> for more details). Daily rainfall, air temperature, and wind speed and direction measurements
334 were recorded at the Abidjan Felix Houphouet Boigny Airport. Figure 1 gives the geographical location of the
335 meteorological station and ambient sampling locations.

337

338 3. Results and discussion

339 3.1 Local meteorological conditions

340 Meteorological data from Abidjan, Côte d'Ivoire, are reported in Figure 2. Weekly accumulated precipitation and
341 weekly air temperature means were analysed during 2016. Meteorological conditions in Abidjan are also affected by
342 the monsoon phenomenon which establishes two well defined seasons: a wet season between March and August and
343 a dry season from November to February. The weekly mean air temperature observed was between 24.6 and 29.4°C,
344 reaching a maximum during the beginning of the wet season (Figure 2). The precipitation pattern shows an increased
345 rate during the monsoon period; however, negative anomalies were observed this year compared with the previous

346 ones (Knippertz et al., 2017). Observed wind patterns during the field campaign showed a predominant contribution
347 from the southwesterly sector with maximum speed during daytime up to 13 m s^{-1} . The high wind speed records
348 reported in Abidjan are higher than those observed in other polluted urban atmospheres (Dominutti et al., 2016;
349 Salameh et al., 2016a; Zhang et al., 2014).

350

351 3.2 VOCs in Abidjan atmosphere

352 Our analysis relies on the fifteen VOC species already listed in Keita et al. (2018, only for emission sources) and
353 these were measured in both ambient air and at emission sources. The VOCs include 8 aromatic hydrocarbons, 3
354 monoterpenes, 3 alkanes, and isoprene which span a wide range of reactivity and represent the various types of VOC
355 expected to be released by fossil/non-fossil fuel combustion and biogenic emissions.

356

357 3.2.1. Ambient concentrations and spatial distribution

358 The ambient concentration sum of the fifteen quantified VOCs ranged from 6.25 to $72.13 \mu\text{g m}^{-3}$ (see size-coded pie
359 chart, Figure 3). Higher VOC concentrations were reported in KSI, BIN CRE and PL sites (Figure 3). The
360 predominant VOCs are toluene ($4.18 \pm 3.55 \mu\text{g m}^{-3}$), m+p-xylene ($4.05 \pm 3.41 \mu\text{g m}^{-3}$), iso-octane ($2.59 \pm 3.37 \mu\text{g}$
361 m^{-3}), benzene ($1.00 \pm 0.41 \mu\text{g m}^{-3}$), ethylbenzene ($0.93 \pm 0.86 \mu\text{g m}^{-3}$) and limonene ($0.77 \pm 0.76 \mu\text{g m}^{-3}$). Overall,
362 anthropogenic VOCs dominated the ambient composition by a factor of 5 to 20 compared to biogenic ones. BTEX
363 (benzene, toluene, ethylbenzene, and m+p and o-xylenes), a subgroup of aromatic VOCs, usually makes up a
364 significant fraction of the VOC burden in urban atmosphere (Borbon et al., 2018; Boynard et al., 2014; Dominutti et
365 al., 2016). They are emitted by fossil fuel combustion from transport and residential sources as well as evaporation
366 processes such as fuel storage and solvent uses (Borbon et al., 2018). Here their contribution ranged from 35% to
367 76% of the total VOC burden measured at the ambient sites. Therefore, the following discussion will only focus on
368 BTEX as representative of all measured anthropogenic VOC patterns. Figure 3 shows the spatial distribution of the
369 total VOC concentrations at each site and detailed by the BTEX composition. Firstly, a spatial heterogeneity of the
370 total measured VOC concentration (total values on pie chart, Figure 3) is depicted in the Abidjan district. This spatial
371 heterogeneity has been already pointed out by recent studies performed in Abidjan for other atmospheric pollutants
372 (Bahino et al., 2018; Djossou et al., 2018). While a spatial heterogeneity was also observed in aerosol concentrations
373 (Djossou et al., 2018), maximum aerosol concentrations were reported near domestic fires (similar to KSI) and
374 landfill sites (AD), showing a different pattern than the one observed for the VOC concentrations. Besides the dilution
375 processes, the spatial distribution of total VOC concentrations seems to be related to the proximity of emission
376 sources, affecting ambient VOC concentrations in the different sampling locations. For example, higher total VOC
377 concentrations were mainly observed in the central urban area (like KSI, CRE and PL) where the density of emission
378 sources increases.

379 Second, m+p-xylene and toluene dominate the ambient distribution of BTEX, ranging from 9 to 27 % and 8 to 31 %
380 of the total VOC, respectively. BTEX composition is consistent between PL, CRE, BIN and KSI sites with high VOC
381 loads while an enrichment in benzene concentrations is observed at FAC, ABO, ZYOP, AT and AD sites (from 16%
382 to 30% contribution). The BTEX composition can be affected by emissions and chemistry. The toluene-to-benzene
383 ratio is a useful indicator of either traffic and non-traffic source or chemistry effects. On the one hand, the toluene-
384 to-benzene at PL, CRE, BIN and KSI sites is higher than 4 which suggests the influence of sources other than traffic

385 like industrial sources. On the other hand, the toluene-to-benzene lie between 0.8 and 1.9 at lower VOC load sites
386 (FAC, ABO, ZYOP, AT and AD) (Brocco et al., 1997; Heeb et al., 2000; Muezzinoglu et al., 2001). These values
387 are closer to the one usually observed at traffic emissions. There is no visible effect of chemistry here especially on
388 higher aromatics like C8-aromatics with a shorter lifetime whose contribution stays almost constant regardless of the
389 site.

390 The mean ambient concentrations observed in Abidjan for alkanes and aromatics were compared with those observed
391 in other cities worldwide (Figure 4). On one hand, mean concentrations in Abidjan depicted lower values when
392 compared with those measured in other cities (Figure 4). Keita and co-workers (2018) pointed out the high emissions
393 observed in Abidjan sources. In their study, road transport and wood burning VOC emission factors spanned 2 to 100
394 orders of magnitude, respectively, when compared with those from the literature. Our ambient observations suggest
395 that wind speed have an important role in the mixing and dilution of the anthropogenic emissions leading to low
396 VOC concentrations in the Abidjan atmosphere. As it was pointed out in the meteorological description, the proximity
397 of Abidjan to the ocean and the intrusion of the sea-breeze circulation can facilitate the dispersion processes and,
398 consequently, the urban emissions dilution. Indeed, Deroubaix et al. (2019) analysed the regional dispersion of urban
399 plumes from SWA coastal cities, i.e. Abidjan, where the inland northward transport of anthropogenic coastal
400 pollutants along with biomass burning emissions were observed.

401 On the other hand, a reasonably good agreement in the relative composition of alkanes and aromatics is observed,
402 showing the same distribution in most cities, except for Karachi where higher contributions of heptane and benzene
403 were measured (Barletta et al., 2002). Observed concentrations of hydrocarbons result from primary emissions,
404 chemical processing and dilution in the atmosphere. Dilution affects equally all the compounds by decreasing
405 absolute levels without altering their composition. Chemistry can be neglected because the transport time between
406 major urban sources and receptor sites is usually less than the compound lifetimes (here the shortest lifetime for
407 trimethylbenzene is 4.3h). Finally, only emissions are expected to significantly alter the hydrocarbon composition.
408 However, the composition is the same regardless of the location. Such commonality suggests that the urban
409 hydrocarbon composition worldwide is controlled by emissions from fossil fuel combustion and, gasoline powered
410 vehicle in particular (see also next section). Finally, the ambient hydrocarbon distributions in Abidjan are noticeably
411 similar to other northern mid-latitude megacities, suggesting that emissions from fossil fuel combustion for alkanes
412 and aromatics dominate over other regional-specific sources. These results are also consistent with previous studies
413 comparing different database worldwide without including an African city like Abidjan (Borbon et al., 2002;
414 Dominutti et al., 2016; von Schneidemesser et al., 2010). Even if emissions can be different in intensity (number of
415 vehicles for instance), the hydrocarbon composition seems to be similar in the different urban atmospheres.

416

417 3.2.2. Ambient composition vs. emission source profiles

418 A comparative approach was carried out between ambient and source measurement compositions with the purpose
419 of detecting emission source fingerprints in ambient VOC profiles. Figure 5 shows the relative mass contribution of
420 VOC profiles observed at the nine urban sites together with those obtained from the emission sources. While a
421 noticeable variability in the contribution of emission sources is observed, smoother differences are depicted between
422 the ambient sites. This result reinforces the similar BTEX profiles discussed in the section 3.2.1, where the mixing
423 and dilution process were suggested as the main drivers in the control of ambient emissions. Trimethylbenzenes (124-

424 TMB, 135-TMB, and 123-TMB), mainly observed in road transport emissions, display a dissimilar profile showing
425 higher fractions from sources than ambient sites (Figure 5). These differences might be related to the short lifetime
426 of these compounds (around 4 hours), with a reaction rate ranging from 1.8 to $8.8 \times 10^{-15} \text{ cm}^3 \text{ molecule}^{-1} \text{ s}^{-1}$ (Atkinson
427 and Arey, 2003). Their reactivity implies a faster reaction in the atmosphere and losses of these species from the
428 emission to the receptor.

429 On the other hand, in most of the cases, ambient profiles showed higher contributions of alkanes, monoterpenes and
430 isoprene, likely associated with the contribution from different anthropogenic and biogenic sources. The presence of
431 terpenes and isoprene in the profile of all emission sources is notable, mainly in those associated with domestic
432 burning processes, such as charcoal, waste and wood fuel burnings (Figure 5). The terpene emissions from biomass
433 burning were already identified in several studies as they are common species emitted by combustion processes
434 (Gilman et al., 2015; Simpson et al., 2011). Additional studies based on African biomass emissions also reported
435 concentrations of limonene and α -pinene higher than isoprene (Jaars et al., 2016; Saxton et al., 2007).

436 For the selected VOC species, aromatic compounds represent the higher fraction from ambient and source profiles,
437 contributing from 31 to 75% (Figure 5). Comparing the same VOC species in emission sources versus ambient
438 profiles, we found a similarity with the two-wheelers and domestic fires profiles like FW and CH sources.
439 Nevertheless, the VOC ambient profiles obtained from the sites did not show a contrasted difference despite the
440 differences in the activities conducted nearby.

441

442 3.3. Molar mass of measured VOC emissions in Abidjan.

443 Here we compare the composition and magnitude of anthropogenic emissions as a function of molar mass emission
444 ratios as described in section 2.3.2, which is a readily calculated property used to quantify anthropogenic emissions
445 (Gilman et al., 2015). For this analysis, our expanded VOC database of 56 species was considered, including 12
446 terpenes, VOCs of intermediate volatility (IVOCs from C_{12} – C_{16} n-alkanes), ketones and aldehydes compounds for
447 all sources (Table 1 and Table S1). Species groups were classified according to GEIA groups (Huang et al., 2017)
448 according to the chemical function of each VOC family (Table S2). In this way, molar masses were also grouped by
449 VOC family from individual values (Table S1). Since the VOCs of intermediate volatility (IVOCs) do not have a
450 specific classification, they were integrated in the group of heavy alkanes (VOC6). **Note also that the most volatile**
451 **fraction of OVOC which usually represents the major fraction, is not represented here in the VOC22 and VOC23**
452 **categories. The associated contribution should be analysed as the lower expected limit.** Figure 6 shows the
453 contribution of VOC groups to the measured molar mass and the total molar mass of each source, while Figure 7a-d
454 (upper panel) compared the magnitude of measured molar masses for the four leading sectors. As already described
455 in the previous section, the distribution reported in Figure 6 reveals the predominance of aromatic molar masses
456 (VOC13-VOC17), ranging from 26 % to 98 %. The prevalence of these compounds is predominantly observed in
457 gasoline-fuelled vehicles, like LDGV and TW sources and diesel light-duty vehicles (LDDV). Alkanes
458 (VOC5+VOC6) also comprise a noticeable molar mass fraction, dominating in TW2T, HDDV and charcoal related
459 sources (by 40, 47 and 53%, respectively).

460 A considerable IVOCs contribution from the emission of HDDV sources was observed, with IVOCs dominating the
461 VOC6 fraction by 30% (considering that VOC6 represents 47% of the total emissions from this source).

462 Interestingly, and as already discussed in Section 3.2.2, monoterpenes (VOC11) comprised 11%, 13% and 22%
463 contribution in FW, HDDV and WB sources, respectively (Figure 6 and Figure 7b-c). Terpenes in biomass burning
464 sources were already pointed out as the most significant emitted compounds together with furans and aromatics in
465 chamber experiments (Koss et al., 2018). Nevertheless, to the extent of our knowledge, their presence in road
466 transport or open waste burning emissions remains unexplored. Regarding OVOCs (VOC22), they were observed in
467 a smaller fraction (less than 7%) apart from HDDV, which contributes to 11% of the total measured molar mass.
468 Previous studies have reported OVOCs as the main fraction in biomass burning emissions (Akagi et al., 2011; Gilman
469 et al., 2015; Yokelson et al., 2013). Moreover, Sekimoto and co-workers also analysed the VOC emission profiles
470 depending on the pyrolysis temperature, showing enrichment of terpenes and non-aromatic oxygenates under high-
471 temperature conditions and an increase in oxygenated aromatics under low-temperature fires (Sekimoto et al., 2018).
472 Comparing the burning-related sources such as FW with previous studies, a lower total measured molar mass was
473 observed in our study than those obtained in the US fuels, by a factor of 33 to 117 (Gilman et al., 2015). In that work,
474 Gilman and co-workers have shown that OVOCs represent 57 to 68% of the total measured molar mass. A different
475 pattern is observed in this study, likely related to the limitation of VOC species measurements by the sampling
476 method deployed, which allows the collection of a limited number of aldehydes ($>C_6$) and other oxygenated
477 compounds as well. Thus, our total molar mass estimation for the sources in Abidjan should be considered as lower
478 limit since additional contributions could be expected from other unknown emitted VOCs, such as OVOCs, alkenes
479 and nitrogenated VOCs.

480 Four sources (TW2T, HDDV, WB, and CH) that represent the leading sectors in the region (road transportation,
481 waste burning, and charcoal burning emissions) were selected, in order to analyse the magnitude of emissions as a
482 function of molar mass and their potential impacts related to African emissions (next section). Figure 7 (a-d) shows
483 the relative composition and the total molar mass of the measured VOC ($\mu\text{g m}^{-3}$) emitted per ppmv of CO. TW2T
484 sources disclosed the highest molar mass emissions ($4680 \pm 512 \mu\text{g m}^{-3} \text{ppmv CO}^{-1}$, Figure 7a-d). TW2T emissions
485 were 10 to 200 times higher than any other source here analysed, such as heavy-duty vehicles (HDDV, $458 \pm 60 \mu\text{g}$
486 $\text{m}^{-3} \text{ppmv CO}^{-1}$), wood burning (FW $31.5 \pm 2.50 \mu\text{g m}^{-3} \text{ppmv CO}^{-1}$), charcoal burning (CH, $43.8 \pm 6.37 \mu\text{g m}^{-3} \text{ppmv}$
487 CO^{-1}) and light-duty vehicles (LDGV, $137.5 \pm 20 \mu\text{g m}^{-3} \text{ppmv CO}^{-1}$) emissions (Figure 6).

488 While aromatics (VOC13-VOC17) seem to dominate the molar mass fraction for most sources, their contributions
489 are dissimilar, dominated by benzene (VOC13) and toluene (VOC14) in burning-related sources, and by xylenes
490 (VOC15) and trimethylbenzenes (VOC16) in traffic-related ones.

491

492 3.4 Implications on atmospheric reactivity

493 The estimation of the impact on atmospheric chemistry of measured VOC emissions is based in the three metrics
494 described in the Section 2.3.

495

496 3.4.1 OH reactivity of measured VOC emissions

497 Figure 7(e-h) shows the fractional contributions and total VOC-OH reactivity per ppmv of CO for the selected
498 sources. The highest total reactivity is observed from the emissions of TW2T ($488 \pm 43 \text{s}^{-1} \text{ppmv CO}^{-1}$), outpacing
499 other sources by a factor of 7 to 170. This disclosed difference is related to the high ERs observed for the more
500 reactive species, like terpenes (VOC11) and C₈- and C₉-aromatics (VOC15 and VOC16, respectively). Terpenes

501 (VOC11) and aromatics (VOC13-VOC17) altogether are the dominant sink of OH, contributing to 47 to 87% of the
502 total calculated OH reactivity. Individually, terpenes governed the OH reactivity in open waste burning emissions
503 (76%) and heavy-duty diesel vehicles (60%) (Figure 7f-g). When compared with other sources, a singular profile is
504 observed for charcoal burning emissions where aldehydes (VOC22, 13%) and heavier alkanes (VOC6, 28%) have
505 higher contribution than in other emission sources. The modest presence of alkenes in the VOC-OH fractional
506 analysis, well-known for their high reactivity effects, is related to the limitation of the sampling method which does
507 not allow the collection of light alkene species. We might expect a high contribution of alkenes adding to the terpene
508 burden.

509

510 3.4.2 Ozone formation potential of measured VOC emissions

511 Overall, the fractional ozone formation distribution is dominated by aromatics (VOC13 to VOC17) in all sources, by
512 38 to 63%. Alkanes (VOC6) represent a significant contribution in charcoal burning, HDDV, and TW2T, accounting
513 for 45, 28 and 26%, respectively. It is important to note the terpenes (VOC11) contribution, coming not only from
514 burning sources but also from the road transportation sector (Figure 7i-l). Aldehydes (VOC22) are well-known due
515 to their high reactivity in the atmosphere (Atkinson and Arey, 2003; Sommariva et al., 2011), and some of these
516 species have shown a large impact on ozone formation and chemistry. In our estimation, we can observe the
517 contribution of these compounds mainly from diesel (HDDV) and charcoal burning sources (CH). The total potential
518 ozone was calculated for each source, showing most of the time a dominant contribution from TW2T (80 343 POCP
519 ppmv CO⁻¹), which is 13, 24 and 150 times higher than the potential impact in ozone formation derived from HDDV,
520 WB and CH emissions, respectively.

521

522 3.4.3 SOA formation potential of measured VOC emissions

523 Figure 7 (m-p) shows the composition and mean SOA formation potentials of VOC families emitted by each selected
524 source. As can be expected, charcoal burning has the lowest SOAP values (335 SOAP per ppmv CO⁻¹), compared
525 with TW2T, HDDV and WB sources, whose SOAPs values are 147, 10 and 9 times greater, respectively. Globally,
526 aromatics (VOC13-VOC17) governed the SOA formation in our estimations, by 72 to 98%. Interestingly, terpenes
527 (VOC11) represented a minor contribution in the SOA formation, presenting a SOAP index lower than for aromatic
528 species. It represents approximately 20% of the SOAP for toluene (VOC14). Despite the well-known role of terpenes
529 as SOA precursors (Ait-Helal et al., 2014), the method used here is not able to correctly quantify their contributions
530 to SOA formation. The differences between SOAP values and measured aerosols yield were already pointed out by
531 Gilman and co-authors (Gilman et al., 2015), who performed some sensitivity tests in order to harmonize SOAP and
532 aerosols yields. We performed the same analysis here, adjusting the SOAP terpene values to be 10% higher. The
533 results in total SOAP per ppmv of CO did not show considerable increases in any of the sources, expanding the total
534 SOAP up to 1%. Similar results were observed for fractional distribution, so that the changes in terpenes SOAPs
535 (VOC11) did not show any substantial change in the VOC contribution for SOA formation. These findings are in
536 agreement with those identified in the study of Gilman et al. (2015), suggesting an underestimation in the fractional
537 contribution of terpenes to the potential formation of organic aerosols over SWA region.

538

539 3.5 Quantification of VOC emissions

540 Anthropogenic VOC emissions were quantified by considering the complete VOC dataset, which includes the 56
541 compounds analysed, aldehydes, IVOCs and terpenes species. Mean residential emissions are also integrated and
542 compared with those from the EDGAR v4.3.2 inventory. Additionally, we incorporate the residential and road
543 transport profiles provided by the MACCity inventory (Granier et al., 2011), available in the ECCAD-GEIA database
544 (<http://eccad.aeris-data.fr>). The main differences between both global inventories are related to the speciation level
545 of VOCs families. MACCity considers all the aromatics in the same VOC group; thus, we provide here the sum of
546 VOC13 to VOC17 families (Table S2) to compare it with the aromatics group from our quantification.

547 Figure 8 exhibits the speciated emissions calculated for Côte d'Ivoire along with those provided by the two emission
548 inventories. Globally, the discrepancies already highlighted in the previous analysis are exacerbated by introducing
549 the complete VOC database. Calculated residential emissions are greater by a factor of 14 and 43 when compared
550 with EDGAR v4.3.2 and MACCity, respectively (Figure 8a). In terms of composition, the main differences observed
551 are related to the VOC22 group (aldehydes). This group discloses a higher contribution by a factor of 5 in the EDGAR
552 inventory, accounting for 64% of the total emission. There is also a disparity in the contribution from aromatics (sum
553 of VOC13 to VOC17) and alkenes (VOC12), which reveals a more substantial influence in the MACCity profile
554 (58% and 22%, respectively) (Figure 8a). This disparity could be related to the few VOC species that were analysed
555 for the VOC12 group in our study. Nevertheless, aromatics dominate the fractional contribution in our calculated
556 emissions (39%), especially toluene (VOC14) and C₈-aromatics (VOC15) (11% and 10%, respectively). Alkanes
557 (>VOC6 alkanes) show a more significant contribution in the residential profile, in which IVOCs contribute 20% of
558 the total calculated alkanes obtained by our estimations.

559 Regarding the road transportation sector, total calculated emissions are higher than the global inventories by a factor
560 of 100 and 160 for EDGAR and MACCity, respectively (Figure 8a). A moderate agreement is observed with
561 speciation (Figure 8b). Aromatics and alkanes are the main contributions for all profiles in different proportions. Our
562 estimates report the most significant contributions in C₈-aromatics (VOC15), C₉-aromatics (VOC16) and toluene
563 (VOC14), with a 25, 14 and 10% contribution, respectively (Figure 8c and Figure 9). In comparison, EDGAR v4.3.2
564 shows a contribution of 9% for VOC15, 3.5% for VOC16 and 13% for VOC14 (Figure 9). Road transport profiles
565 also reproduce the anomalies in the VOC12 (alkenes) contribution observed in the residential sector, presenting
566 greater emissions in the global inventories. The comparison between both inventories also depicted considerable
567 discrepancies, of a factor of 3.

568 A similar profile is observed for heavier alkanes (VOC6) which present an analogous contribution between our
569 estimation and EDGAR emissions (34 and 37%, respectively; Figure 8b). Nevertheless, the alkanes (VOC5+VOC6)
570 contribution in the MACCity profiles prevails over road transport emissions accounting for 62% of the total
571 emissions.

572 Interestingly, terpenes and isoprene emissions can be denoted in both sectors in the Côte d'Ivoire calculated emissions
573 (VOC11 and VOC10). Despite the reduced contribution of these species (9% in residential and 4% in road transport),
574 the underestimation of them in the emissions from anthropogenic sources could have consequences for atmospheric
575 chemistry. Since the reactivity is specific for each VOC, the inaccuracies in the speciation could also have
576 implications on the estimation of their impacts. Specifically for terpenes (VOC11), it can be noted their high
577 contribution in the k_{OH} reactivity, accounting for 42% in the residential sector and 28% in road transport sector

578 reactivities (Figure 8c). Even though the total OH reactivity in all profiles is rather similar, the alkenes fraction in
579 this study is not well-represented which could increase the contribution in terms of reactivity.

580 Figure 9 also displays the residential and road transportation profiles obtained from Côte d'Ivoire, compared with
581 EDGAR v4.3.2 profiles for Europe. Noticeably in our estimations, road transport and residential sectors presented
582 comparable total emissions, whereas those from the EDGAR inventory were different by a factor of 8 (86.1 vs 12.1
583 Gg year⁻¹, respectively). Similar disagreements are also observed when comparing EDGAR total emissions for
584 Europe with Côte d'Ivoire, where the former presents larger emissions (198 vs 86 and 433 vs 12 Gg year⁻¹,
585 respectively). We highlight here the substantial differences in total emissions, outpacing those estimated for Europe
586 by a factor of 3 for road transport and by a factor of 6 for residential sector (433 and 198 Gg year⁻¹, respectively).

587 The lack of measurements and source profile data in Africa was previously pointed out in the development of EDGAR
588 inventory, which led to considering the priority of this region for future inventory improvements (Huang et al., 2017).
589 Even though our VOC database is not extensive for all the species emitted by the sources analysed, the incorporation
590 of new VOC species reinforces the usefulness of *in situ* measurements under real conditions to derive realistic
591 emission factors and subsequent estimates of representative emission profiles.

592

593 3.6 Anthropogenic emissions of terpenes, IVOCs and aldehydes in SWA

594 As previously highlighted, terpenes commonly emitted by biogenic sources were observed in the emissions from
595 anthropogenic sources. Global emission inventories wholly neglect these emissions; however, they could have
596 considerable effects in the atmospheric chemical processing, by producing secondary pollutants in the atmosphere.
597 Figure 10a shows the fractional distribution of terpenes in several analysed emission sources. The main contributions
598 are associated with the emissions from waste burning (WB, 47%), two-wheel vehicles (TW2T, 20%), wood burning
599 (FW, 17%) and charcoal making (CHM, 14%) sources. The total annual emissions estimated for these compounds,
600 which represents 334 Gg year⁻¹ and 11% of the total emissions, cannot be neglected when compared with the emission
601 of other well-known anthropogenic VOC, i.e. C₉-aromatics. Evaluating the distribution of terpene species among the
602 emission sources permits a different pattern to be noted (Figure 11). While terpene emissions from road transport are
603 mainly dominated by α -ocimene and α -terpinolene, limonene and isoprene are mainly emitted by wood-burning
604 sources. The main wood types burnt in Côte d'Ivoire are Hevea (*Hevea brasiliensis*) and Iroko (*Milicia excelsa*),
605 which are widely used in urban domestic fires for cooking, heating and other services (Keita et al., 2018). In our
606 study, we only present the results obtained from Hevea, a tropical African hardwood, characterised as a species that
607 emits monoterpenes (Bracho-Nunez et al., 2013; Wang et al., 2007). The principal monoterpene compounds naturally
608 emitted by Hevea species are sabinene, limonene, and α -pinene (Bracho-Nunez et al., 2013). The isoprene emissions
609 from non-isoprene emitting species were already observed in biomass burning studies, which indicates that isoprene
610 is formed during the combustion process (Hatch et al., 2015).

611 As it can be noted in Figure 11, isoprene emissions are also impacted by vehicles, mainly TW sources, and camphene
612 and β -pinene emissions by HDDV sources. The anthropogenic sources of isoprene have been documented in urban
613 areas, mainly associated with traffic emissions (Borbon et al., 2001; von Schneidmesser et al., 2011). However, to
614 the best of our knowledge, no previous studies have ever analysed the presence of monoterpenes from road
615 transportation sources. α -pinene and β -pinene emissions are dominated by charcoal burning fires, which also
616 contribute in some fraction to the emissions of isoprene and limonene. In contrast, charcoal making emissions are

617 dominated by γ -terpinene and isoprene. The results from biomass burning sources provided here were obtained from
618 non-controlled experiments, which did not allow the evaluation of differences between the emissions from each
619 combustion phase (pyrolysis, flaming and smouldering). Further investigation is needed in order to develop a better
620 understanding of these differences and to characterize the different combustion phases.

621 VOCs of intermediate volatility are suspected to be efficient precursors of SOA (Seinfeld and Pandis, 2006 and
622 references therein). However, as it was discussed in the section 3.4.3, our method was not able to resolve the
623 differences between VOC families and most SOA was assigned to aromatic compounds (up to 98%). Figure 10b
624 reports the fractional contribution and total emissions of IVOCs. CHM, FW, HDDV, and TW represent the primary
625 sources of these compounds, accounting for 58, 15, 12 and 11% of the total, respectively. Despite their lower
626 emissions compared with aromatics or terpenes, IVOCs are estimated to account for 80 Gg year⁻¹ of emissions in
627 Côte d'Ivoire. A recent study observed that fine particles in Abidjan are three times higher than the World Health
628 Organization recommended concentrations (Djossou et al., 2018). Hence, a better understanding of the aerosol
629 precursors and formation processes is essential for the later reduction of their concentrations in the urban atmosphere.
630 Oxygenated compounds were previously indicated as essential species in the emissions from burning sources
631 (Gilman et al., 2015; Hatch et al., 2015; Koss et al., 2018; Wiedinmyer et al., 2014). In addition, oxygenated
632 compounds like non-aromatics were dominant in the burning emission sources including a range of functional groups,
633 of which alcohols and carbonyls were the most abundant (Koss et al., 2018; Stockwell et al., 2015). Figure 10c
634 shows that aldehyde emissions are mainly governed by charcoal fabrication (CHM), two-wheel vehicles (TW) and
635 wood burning sources (Figure 10c). In our study the quantified aldehydes represent only 5.5% of the total emissions
636 of the country (170 Gg year⁻¹). However, they can be essential compounds concerning reactivity and ozone formation.
637 Hence, further analysis of oxygenated compounds together with furans and other nitro-oxygenated compounds needs
638 to be addressed in future campaigns, in order to improve not only the quantification of these compounds but also
639 provide a better identification of the African tracers from biomass burning processes.

640

641 4. Summary and conclusions

642 This study reports for the first time a chemically detailed range of VOCs including C₅-C₁₆ alkanes, monoterpenes,
643 alkenes, aromatics and carbonyls compounds by using sorbent tubes during an intensive field campaign in Abidjan,
644 SWA. We present here an original dataset integrating main emission sources and ambient measurements from nine
645 representative sites, and covering the urban spatial distribution of VOCs in Abidjan. The spatial distribution and
646 composition of VOC in ambient air in Abidjan reveals the effect of local burning and traffic emissions. The highest
647 concentrations were observed near domestic fires, landfill fires and traffic sites, in agreement with the results reported
648 in previous studies, when gas-phase and aerosols pollutants were measured (Bahino et al., 2018; Djossou et al., 2018).
649 The calculation of emission ratios is an important metric to evaluate the estimates provided by global emission
650 inventories. Emission ratios from regional-specific emission sources were established here and later used for the
651 analysis of fractional molar mass contribution and the estimation of potential VOC OH reactivity, ozone and
652 secondary organic aerosol formation. The distribution of VOC emissions (magnitude and composition) was different
653 for each evaluated source. Two wheel and heavy-duty vehicle sources presented the most significant total molar mass
654 emissions, while charcoal-burning was the lowest. The sources related to burning processes, such as waste and wood

655 burning, also presented significant contribution to VOCs emissions. These sources represent common activities
656 present in Abidjan and might contribute a large quantity of VOC emissions to the SWA region.

657 Regarding VOC speciation, molar mass contributions were mostly dominated by aromatic and alkane compounds.
658 Since few alkene species were quantified, aromatics ruled both ozone and SOA formation potential. However, the
659 SOA metrics applied here were not able to accurately analyse the other important SOA precursors contribution, such
660 as monoterpenes. Nevertheless, monoterpenes can contribute significantly to VOC OH reactivity from some sources
661 like WB, and the alkane species can significantly contribute to the total reactivity.

662 In order to estimate the magnitude of VOC emissions in Côte d'Ivoire, emission factors were determined from the
663 *in-situ* VOC database. Road transportation and residential profiles were obtained and compared with those reported
664 in global emission inventories (MACCcity and EDGAR). Our results revealed a discrepancy of up to a factor of 43
665 and 160 for residential and transport profiles when compared with both referenced inventories. The high levels of
666 VOC emissions obtained for Côte d'Ivoire outpace European emissions by up to a factor of 6. Interestingly,
667 monoterpene emissions were observed in anthropogenic emission sources from biomass burning to road
668 transportation sources, contributing to up to 340 Gg year⁻¹. These compounds are generally missing in the global
669 anthropogenic emission profiles, which would underestimate their impacts on air quality. This underestimation is not
670 only expected for Côte d'Ivoire but for all West Africa countries.

671 This study, in the framework of the DACCIWA project, allowed us for the first time to identify and quantify several
672 VOCs in ambient air and at emission sources in Abidjan, Côte d'Ivoire. Our results provide significant constraints
673 for the development of more realistic regional emission inventories. A continuous effort is needed to collect new
674 emission data and ambient measurements in West African countries for all critical atmospheric pollutants.

675

676 **Acknowledgments**

677 This work has received funding from the European Union Seventh Framework Programme (FP7/2007-2013) under
678 grant agreement number 603502 (EU project DACCIWA: Dynamics-aerosol-chemistry-cloud interactions in West
679 Africa). P Dominutti acknowledges the Postdoctoral Fellowship support from the Université Clermont Auvergne and
680 thanks the grant received from the CAPES program (Process N°: 88887.098995/2015-00, CAPES – PVE's Program,
681 2014) from the Ministry of Education of Brazil, during 2015-2016. Thierry Leonardis is thanked for the contribution
682 in the analysis of VOC sorbent tubes, graciously performed at the SAGE Department at IMT Lille Douai (France).

683

684 *Data availability.*

685 All data used in this study is available on the AERIS Data and Service Center, which can be found at
686 <http://baobab.sedoo.fr/DACCIWA>.

687

688 *Competing interests.* The authors declare that they have no conflict of interest.

689

691 **References**

- 692 AIRPARIF: Surveillance de la qualite de l'air en Ile-de-France., [online] Available from: <http://www.airparif.asso.fr/>
693 (Accessed 1 March 2018), 2016.
- 694 Ait-Helal, W., Borbon, A., Sauvage, S., de Gouw, J. A., Colomb, A., Gros, V., Freutel, F., Crippa, M., Afif, C.,
695 Baltensperger, U., Beekmann, M., Doussin, J.-F., Durand-Jolibois, R., Fronval, I., Grand, N., Leonardis, T., Lopez, M.,
696 Michoud, V., Miet, K., Perrier, S., Prévôt, A. S. H., Schneider, J., Siour, G., Zapf, P. and Locoge, N.: Volatile and
697 intermediate volatility organic compounds in suburban Paris: variability, origin and importance for SOA formation, *Atmos.*
698 *Chem. Phys.*, 14(19), 10439–10464, doi:10.5194/acp-14-10439-2014, 2014.
- 699 Akagi, S. K., Yokelson, R. J., Wiedinmyer, C., Alvarado, M. J., Reid, J. S., Karl, T., Crounse, J. D. and Wennberg, P. O.:
700 Emission factors for open and domestic biomass burning for use in atmospheric models, *Atmos. Chem. Phys.*, 11(9), 4039–
701 4072, doi:10.5194/acp-11-4039-2011, 2011.
- 702 Assamoi, E.-M. and Liousse, C.: A new inventory for two-wheel vehicle emissions in West Africa for 2002, *Atmos.*
703 *Environ.*, 44(32), 3985–3996, doi:10.1016/j.atmosenv.2010.06.048, 2010.
- 704 Atkinson, R. and Arey, J.: Atmospheric Degradation of Volatile Organic Compounds, *Chem. Rev.*, 103(12), 4605–4638,
705 doi:10.1021/cr0206420, 2003.
- 706 Bahino, J., Yoboué, V., Galy-Lacaux, C., Adon, M., Akpo, A., Keita, S., Liousse, C., Gardrat, E., Chiron, C., Ossohou, M.,
707 Gnamien, S. and Djossou, J.: A pilot study of gaseous pollutants' measurement (NO₂, SO₂, NH₃, HNO₃ and O₃) in
708 Abidjan, Côte d'Ivoire: contribution to an overview of gaseous pollution in African cities, *Atmos. Chem. Phys.*, 18(7),
709 5173–5198, doi:10.5194/acp-18-5173-2018, 2018.
- 710 Baker, A. K., Beyersdorf, A. J., Doezema, L. a., Katzenstein, A., Meinardi, S., Simpson, I. J., Blake, D. R. and Sherwood,
711 F. R.: Measurements of nonmethane hydrocarbons in 28 United States cities, *Atmos. Environ.*, 42(1), 170–182,
712 doi:10.1016/j.atmosenv.2007.09.007, 2008.
- 713 Barletta, B., Meinardi, S., Simpson, I. J., Khwaja, H. a, Blake, D. R. and Rowland, F. S.: Mixing ratios of volatile organic
714 compounds (VOCs) in the atmosphere of Karachi, Pakistan, *Atmos. Environ.*, 36(21), 3429–3443, doi:10.1016/S1352-
715 2310(02)00302-3, 2002.
- 716 Bechara, J., Borbon, A., Jambert, C., Colomb, A. and Perros, P. E.: Evidence of the impact of deep convection on reactive
717 Volatile Organic Compounds in the upper tropical troposphere during the AMMA experiment in West Africa, *Atmos.*
718 *Chem. Phys.*, 10(21), 10321–10334, doi:10.5194/acp-10-10321-2010, 2010.
- 719 Bon, D., Ulbrich, I. and de Gouw, J. A.: Measurements of volatile organic compounds at a suburban ground site (T1) in
720 Mexico City during the MILAGRO 2006 campaign: measurement comparison, emission, *Atmos. Chem. Phys.*, 2011.
- 721 Borbon, A., Fontaine, H., Veillerot, M., Locoge, N., Galloo, J. C. and Guillermo, R.: An investigation into the traffic-
722 related fraction of isoprene at an urban location, *Atmos. Environ.*, 35(22), 3749–3760, doi:10.1016/S1352-2310(01)00170-
723 4, 2001.
- 724 Borbon, A., Locoge, N., Veillerot, M., GALLOO, J. C. and GUILLERMO, R.: Characterisation of NMHCs in a French
725 urban atmosphere: overview of the main sources, *Sci. Total Environ.*, 292(3), 177–191, doi:10.1016/S0048-
726 9697(01)01106-8, 2002.
- 727 Borbon, A., Gilman, J. B., Kuster, W. C., Grand, N., Chevaillier, S., Colomb, A., Dolgorouky, C., Gros, V., Lopez, M.,
728 Sarda-Esteve, R., Holloway, J., Stutz, J., Petetin, H., McKeen, S., Beekmann, M., Warneke, C., Parrish, D. D. and de

729 Gouw, J. A.: Emission ratios of anthropogenic volatile organic compounds in northern mid-latitude megacities:
730 Observations versus emission inventories in Los Angeles and Paris, *J. Geophys. Res. Atmos.*, 118(4), 2041–2057,
731 doi:10.1002/jgrd.50059, 2013.

732 Borbon, A., Boynard, A., Salameh, T., Baudic, A., Gros, V., Gauduin, J., Perrussel, O. and Pallares, C.: Is Traffic Still an
733 Important Emitter of Monoaromatic Organic Compounds in European Urban Areas?, *Environ. Sci. Technol.*, 52(2), 513–
734 521, doi:10.1021/acs.est.7b01408, 2018.

735 Boynard, A., Borbon, A., Leonardis, T., Barletta, B., Meinardi, S., Blake, D. R. and Locoge, N.: Spatial and seasonal
736 variability of measured anthropogenic non-methane hydrocarbons in urban atmospheres: Implication on emission ratios,
737 *Atmos. Environ.*, 82, 258–267, doi:10.1016/j.atmosenv.2013.09.039, 2014.

738 Bracho-Nunez, A., Knothe, N. M., Welter, S., Staudt, M., Costa, W. R., Liberato, M. A. R., Piedade, M. T. F. and
739 Kesselmeier, J.: Leaf level emissions of volatile organic compounds (VOC) from some Amazonian and Mediterranean
740 plants, *Biogeosciences*, 10(9), 5855–5873, doi:10.5194/bg-10-5855-2013, 2013.

741 Brito, J., Wurm, F., Yáñez-Serrano, A. M., de Assunção, J. V., Godoy, J. M. and Artaxo, P.: Vehicular Emission Ratios of
742 VOCs in a Megacity Impacted by Extensive Ethanol Use: Results of Ambient Measurements in São Paulo, Brazil, *Environ.*
743 *Sci. Technol.*, 49(19), 11381–11387, doi:10.1021/acs.est.5b03281, 2015.

744 Brocco, D., Fratarcangeli, R., Lepore, L., Petricca, M. and Ventrone, I.: Determination of aromatic hydrocarbons in urban
745 air of Rome, *Atmos. Environ.*, 31(4), 557–566, doi:10.1016/S1352-2310(96)00226-9, 1997.

746 Deroubaix, A., Menut, L., Flamant, C., Brito, J., Denjean, C., Dreiling, V., Fink, A., Jambert, C., Kalthoff, N., Knippertz,
747 P., Ladkin, R., Mailler, S., Maranan, M., Pacifico, F., Piguet, B., Siour, G. and Turquety, S.: Diurnal cycle of coastal
748 anthropogenic pollutant transport over southern West Africa during the DACCIWA campaign, *Atmos. Chem. Phys.*, 19(1),
749 473–497, doi:10.5194/acp-19-473-2019, 2019.

750 Derwent, R. G., Jenkin, M. E., Saunders, S. M. and Pilling, M. J.: Photochemical ozone creation potentials for organic
751 compounds in northwest Europe calculated with a master chemical mechanism, *Atmos. Environ.*, 32(14–15), 2429–2441,
752 doi:10.1016/S1352-2310(98)00053-3, 1998.

753 Derwent, R. G., Jenkin, M. E., Passant, N. R. and Pilling, M. J.: Photochemical ozone creation potentials (POCPs) for
754 different emission sources of organic compounds, *Atmos. Environ.*, 41(12), 2570–2579,
755 doi:10.1016/j.atmosenv.2006.11.019, 2007.

756 Derwent, R. G., Jenkin, M. E., Utembe, S. R., Shallcross, D. E., Murrells, T. P. and Passant, N. R.: Secondary organic
757 aerosol formation from a large number of reactive man-made organic compounds, *Sci. Total Environ.*, 408(16), 3374–
758 3381, doi:10.1016/j.scitotenv.2010.04.013, 2010.

759 Detournay, A., Sauvage, S., Locoge, N., Gaudion, V., Leonardis, T., Fronval, I., Kaluzny, P. and Galloo, J.-C.:
760 Development of a sampling method for the simultaneous monitoring of straight-chain alkanes, straight-chain saturated
761 carbonyl compounds and monoterpenes in remote areas., *J. Environ. Monit.*, 13(4), 983–990, doi:10.1039/c0em00354a,
762 2011.

763 Djossou, J., Léon, J.-F., Akpo, A. B., Liousse, C., Yoboué, V., Bedou, M., Bodjrenou, M., Chiron, C., Galy-Lacaux, C.,
764 Gardrat, E., Abbey, M., Keita, S., Bahino, J., N'Datchoh, E. T., Ossouhou, M. and Awanou, C. N.: Mass concentration,
765 optical depth and carbon composition of particulate matter in the major southern West African cities of Cotonou (Benin)
766 and Abidjan (Côte d'Ivoire), *Atmos. Chem. Phys.*, 18(9), 6275–6291, doi:10.5194/acp-18-6275-2018, 2018.

767 Dominutti, P. A., Nogueira, T., Borbon, A., Andrade, M. de F. and Fornaro, A.: One-year of NMHCs hourly observations

768 in São Paulo megacity: meteorological and traffic emissions effects in a large ethanol burning context, *Atmos. Environ.*,
769 142, 371–382, doi:10.1016/j.atmosenv.2016.08.008, 2016.

770 Epstein, S. A., Riipinen, I. and Donahue, N. M.: A Semiempirical Correlation between Enthalpy of Vaporization and
771 Saturation Concentration for Organic Aerosol, *Environ. Sci. Technol.*, 44(2), 743–748, doi:10.1021/es902497z, 2010.

772 Gaimoz, C., Sauvage, S., Gros, V., Herrmann, F., Williams, J., Locoge, N., Perrussel, O., Bonsang, B., D'Argouges, O.,
773 Sarda-Estève, R. and Sciare, J.: Volatile organic compounds sources in Paris in spring 2007. Part II: source apportionment
774 using positive matrix factorisation, *Environ. Chem.*, 8(1), 91, doi:10.1071/EN10067, 2011.

775 Gilman, J. B., Lerner, B. M., Kuster, W. C., Goldan, P. D., Warneke, C., Veres, P. R., Roberts, J. M., De Gouw, J. A.,
776 Burling, I. R. and Yokelson, R. J.: Biomass burning emissions and potential air quality impacts of volatile organic
777 compounds and other trace gases from fuels common in the US, *Atmos. Chem. Phys.*, 15(24), 13915–13938,
778 doi:10.5194/acp-15-13915-2015, 2015.

779 de Gouw, J. A., Gilman, J. B., Kim, S.-W., Lerner, B. M., Isaacman-VanWertz, G., McDonald, B. C., Warneke, C., Kuster,
780 W. C., Lefer, B. L., Griffith, S. M., Dusanter, S., Stevens, P. S. and Stutz, J.: Chemistry of Volatile Organic Compounds in
781 the Los Angeles basin: Nighttime Removal of Alkenes and Determination of Emission Ratios, *J. Geophys. Res. Atmos.*,
782 122(21), 11,843–11,861, doi:10.1002/2017JD027459, 2017.

783 Granier, C., Bessagnet, B., Bond, T., D'Angiola, A., Denier van der Gon, H., Frost, G. J., Heil, A., Kaiser, J. W., Kinne, S.,
784 Klimont, Z., Kloster, S., Lamarque, J.-F., Liousse, C., Masui, T., Meleux, F., Mieville, A., Ohara, T., Raut, J.-C., Riahi, K.,
785 Schultz, M. G., Smith, S. J., Thompson, A., van Aardenne, J., van der Werf, G. R. and van Vuuren, D. P.: Evolution of
786 anthropogenic and biomass burning emissions of air pollutants at global and regional scales during the 1980–2010 period,
787 *Clim. Change*, 109(1–2), 163–190, doi:10.1007/s10584-011-0154-1, 2011.

788 Hatch, L. E., Luo, W., Pankow, J. F., Yokelson, R. J., Stockwell, C. E. and Barsanti, K. C.: Identification and quantification
789 of gaseous organic compounds emitted from biomass burning using two-dimensional gas chromatography-time-of-flight
790 mass spectrometry, *Atmos. Chem. Phys.*, 15(4), 1865–1899, doi:10.5194/acp-15-1865-2015, 2015.

791 Heeb, N. V., Forss, A.-M., Bach, C., Reimann, S., Herzog, A. and Jäckle, H. W.: A comparison of benzene, toluene and
792 C2-benzenes mixing ratios in automotive exhaust and in the suburban atmosphere during the introduction of catalytic
793 converter technology to the Swiss Car Fleet, *Atmos. Environ.*, 34(19), 3103–3116, doi:10.1016/S1352-2310(99)00446-X,
794 2000.

795 Huang, G., Brook, R., Crippa, M., Janssens-Maenhout, G., Schieberle, C., Dore, C., Guizzardi, D., Muntean, M., Schaaf, E.
796 and Friedrich, R.: Speciation of anthropogenic emissions of non-methane volatile organic compounds: A global gridded
797 data set for 1970–2012, *Atmos. Chem. Phys.*, 17(12), 7683–7701, doi:10.5194/acp-17-7683-2017, 2017.

798 Jaars, K., Beukes, J. P., Van Zyl, P. G., Venter, A. D., Josipovic, M., Pienaar, J. J., Vakkari, V., Aaltonen, H., Laakso, H.,
799 Kulmala, M., Tiitta, P., Guenther, A., Hellén, H., Laakso, L. and Hakola, H.: Ambient aromatic hydrocarbon measurements
800 at Welgegund, South Africa, *Atmos. Chem. Phys.*, 14(13), 7075–7089, doi:10.5194/acp-14-7075-2014, 2014.

801 Jaars, K., Van Zyl, P. G., Beukes, J. P., Hellén, H., Vakkari, V., Josipovic, M., Venter, A. D., Räsänen, M., Knoetze, L.,
802 Cilliers, D. P., Siebert, S. J., Kulmala, M., Rinne, J., Guenther, A., Laakso, L. and Hakola, H.: Measurements of biogenic
803 volatile organic compounds at a grazed savannah grassland agricultural landscape in South Africa, *Atmos. Chem. Phys.*,
804 16(24), 15665–15688, doi:10.5194/acp-16-15665-2016, 2016.

805 Jenkin, M. E., Derwent, R. G. and Wallington, T. J.: Photochemical ozone creation potentials for volatile organic
806 compounds: Rationalization and estimation, *Atmos. Environ.*, 163(x), 128–137, doi:10.1016/j.atmosenv.2017.05.024, 2017.

807 Keita, S., Liousse, C., Yoboué, V., Dominutti, P., Guinot, B., Assamoi, E.-M., Borbon, A., Haslett, S. L., Bouvier, L.,
808 Colomb, A., Coe, H., Akpo, A., Adon, J., Bahino, J., Doumbia, M., Djossou, J., Galy-Lacaux, C., Gardrat, E., Gnamien, S.,
809 Léon, J. F., Ossohou, M., N'Datchoh, E. T. and Roblou, L.: Particle and VOC emission factor measurements for
810 anthropogenic sources in West Africa, *Atmos. Chem. Phys.*, 18(10), 7691–7708, doi:10.5194/acp-18-7691-2018, 2018.

811 Knippertz, P., Coe, H., Chiu, J. C., Evans, M. J., Fink, A. H., Kalthoff, N., Liousse, C., Mari, C., Allan, R. P., Brooks, B.,
812 Danour, S., Flamant, C., Jegede, O. O., Lohou, F. and Marsham, J. H.: The DACCIWA Project: Dynamics–Aerosol–
813 Chemistry–Cloud Interactions in West Africa, *Bull. Am. Meteorol. Soc.*, 96(9), 1451–1460, doi:10.1175/BAMS-D-14-
814 00108.1, 2015a.

815 Knippertz, P., Evans, M. J., Field, P. R., Fink, A. H., Liousse, C. and Marsham, J. H.: The possible role of local air
816 pollution in climate change in West Africa, *Nat. Clim. Chang.*, 5(9), 815–822, doi:10.1038/nclimate2727, 2015b.

817 Knippertz, P., Fink, A. H., Deroubaix, A., Morris, E., Tocquer, F., Evans, M. J., Flamant, C., Gaetani, M., Lavaysse, C.,
818 Mari, C., Marsham, J. H., Meynadier, R., Affo-Dogo, A., Bahaga, T., Brosse, F., Deetz, K., Guebsi, R., Latifou, I.,
819 Maranan, M., Rosenberg, P. D. and Schlueter, A.: A meteorological and chemical overview of the DACCIWA field
820 campaign in West Africa in June–July 2016, *Atmos. Chem. Phys.*, 17(17), 10893–10918, doi:10.5194/acp-17-10893-2017,
821 2017.

822 Koss, A. R., Sekimoto, K., Gilman, J. B., Selimovic, V., Coggon, M. M., Zarzana, K. J., Yuan, B., Lerner, B. M., Brown,
823 S. S., Jimenez, J. L., Krechmer, J., Roberts, J. M., Warneke, C., Yokelson, R. J. and De Gouw, J.: Non-methane organic gas
824 emissions from biomass burning: Identification, quantification, and emission factors from PTR-ToF during the FIREX
825 2016 laboratory experiment, *Atmos. Chem. Phys.*, 18(5), 3299–3319, doi:10.5194/acp-18-3299-2018, 2018.

826 Kumar, A., Singh, D., Kumar, K., Singh, B. B. and Jain, V. K.: Distribution of VOCs in urban and rural atmospheres of
827 subtropical India: Temporal variation, source attribution, ratios, OFP and risk assessment, *Sci. Total Environ.*, 613–614,
828 492–501, doi:10.1016/j.scitotenv.2017.09.096, 2018.

829 Liousse, C., Assamoi, E., Criqui, P., Granier, C. and Rosset, R.: Explosive growth in African combustion emissions from
830 2005 to 2030, *Environ. Res. Lett.*, 9(3), 035003, doi:10.1088/1748-9326/9/3/035003, 2014.

831 Manion, J. A., Huie, R. E., Levin, R. D., Jr., D. R. B., Orkin, V. L., Tsang, W., McGivern, W. S., Hudgens, J. W., Knyazev,
832 V. D., Atkinson, D. B., Chai, E., Tereza, A. M., Lin, C.-Y., Allison, T. C., Mallard, W. G., Westley, F., Herron, J. T., R. F.
833 Hampson, A. and Frizzell, D. H.: NIST Chemical Kinetics Database, Gaithersburg, Maryland. [online] Available from:
834 <http://kinetics.nist.gov/> (Accessed 18 April 2018), 2015.

835 Mari, C. H., Reeves, C. E., Law, K. S., Ancellet, G., Andrés-Hernández, M. D., Barret, B., Bechara, J., Borbon, A.,
836 Bouarar, I., Cairo, F., Commane, R., Delon, C., Evans, M. J., Fierli, F., Floquet, C., Galy-Lacaux, C., Heard, D. E., Homan,
837 C. D., Ingham, T., Larsen, N., Lewis, A. C., Liousse, C., Murphy, J. G., Orlandi, E., Oram, D. E., Saunois, M., Serça, D.,
838 Stewart, D. J., Stone, D., Thouret, V., Velthoven, P. van and Williams, J. E.: Atmospheric composition of West Africa:
839 Highlights from the AMMA international program, *Atmos. Sci. Lett.*, 12(1), 13–18, doi:10.1002/asl.289, 2011.

840 Muezzinoglu, A., Odabasi, M. and Onat, L.: Volatile organic compounds in the air of Izmir, Turkey, *Atmos. Environ.*,
841 35(4), 753–760, doi:10.1016/S1352-2310(00)00420-9, 2001.

842 Niedojadlo, A., Becker, K. H., Kurtenbach, R. and Wiesen, P.: The contribution of traffic and solvent use to the total
843 NMVOC emission in a German city derived from measurements and CMB modelling, *Atmos. Environ.*, 41(33), 7108–
844 7126, doi:10.1016/j.atmosenv.2007.04.056, 2007.

845 Robinson, A. L., Donahue, N. M., Shrivastava, M. K., Weitkamp, E. a, Sage, A. M., Grieshop, A. P., Lane, T. E., Pierce, J.

846 R. and Pandis, S. N.: Rethinking Organic Aerosols: Semivolatile Emissions and Photochemical Aging, *Science* (80-.),
847 315(5816), 1259–1262, doi:10.1126/science.1133061, 2007.

848 Salameh, T., Afif, C., Sauvage, S., Borbon, A. and Locoge, N.: Speciation of non-methane hydrocarbons (NMHCs) from
849 anthropogenic sources in Beirut, Lebanon, *Environ. Sci. Pollut. Res.*, 21(18), 10867–10877, doi:10.1007/s11356-014-2978-
850 5, 2014.

851 Salameh, T., Sauvage, S., Afif, C., Borbon, A., Léonardis, T., Brioude, J., Waked, A. and Locoge, N.: Exploring the
852 seasonal NMHC distribution in an urban area of the Middle East during ECOCEM campaigns: Very high loadings
853 dominated by local emissions and dynamics, *Environ. Chem.*, 12(3), 316–328, doi:10.1071/EN14154, 2015.

854 Salameh, T., Borbon, A., Afif, C., Sauvage, S., Leonardis, T., Gaimoz, C. and Locoge, N.: Composition of gaseous organic
855 carbon during ECOCEM in Beirut, Lebanon: new observational constraints for VOC anthropogenic emission evaluation in
856 the Middle East, *Atmos. Chem. Phys. Discuss.*, (August), 1–32, doi:10.5194/acp-2016-543, 2016a.

857 Salameh, T., Sauvage, S., Afif, C., Borbon, A. and Locoge, N.: Source apportionment vs. emission inventories of non-
858 methane hydrocarbons (NMHC) in an urban area of the Middle East: local and global perspectives, *Atmos. Chem. Phys.*,
859 16(5), 3595–3607, doi:10.5194/acp-16-3595-2016, 2016b.

860 Saxton, J. E., Lewis, A. C., Kettlewell, J. H., Ozel, M. Z., Gogus, F., Boni, Y., Korogone, S. O. U. and Serça, D.: Isoprene
861 and monoterpene emissions from secondary forest in northern Benin, *Atmos. Chem. Phys. Discuss.*, 7(2), 4981–5012,
862 doi:10.5194/acpd-7-4981-2007, 2007.

863 von Schneidmesser, E., Monks, P. S. and Plass-Duelmer, C.: Global comparison of VOC and CO observations in urban
864 areas, *Atmos. Environ.*, 44(39), 5053–5064, doi:10.1016/j.atmosenv.2010.09.010, 2010.

865 von Schneidmesser, E., Monks, P. S., Gros, V., Gauduin, J. and Sanchez, O.: How important is biogenic isoprene in an
866 urban environment? A study in London and Paris, *Geophys. Res. Lett.*, 38(19), doi:10.1029/2011GL048647, 2011.

867 Seinfeld, J. H. and Pandis, S. N.: *Atmospheric Chemistry and Physics. From Air Pollution to Climate Change*, Second edi.,
868 John Wiley & Sons., 2006.

869 Sekimoto, K., Koss, A. R., Gilman, J. B., Selimovic, V., Coggon, M. M., Zarzana, K. J., Yuan, B., Lerner, B. M., Brown,
870 S. S., Warneke, C., Yokelson, R. J., Roberts, J. M. and de Gouw, J.: High- and low-temperature pyrolysis profiles describe
871 volatile organic compound emissions from western US wildfire fuels, *Atmos. Chem. Phys.*, 18(13), 9263–9281,
872 doi:10.5194/acp-18-9263-2018, 2018.

873 SIE CI: Rapport Côte d'Ivoire Energie 2010., , 57 [online] Available from:
874 http://www.ecowrex.org/system/files/repository/2010_rapport_annuel_sie_-_min_ener.pdf (Accessed 27 August 2018),
875 2010.

876 Simpson, I. J., Akagi, S. K., Barletta, B., Blake, N. J., Choi, Y., Diskin, G. S., Fried, A., Fuelberg, H. E., Meinardi, S.,
877 Rowland, F. S., Vay, S. A., Weinheimer, A. J., Wennberg, P. O., Wiebring, P., Wisthaler, A., Yang, M., Yokelson, R. J.
878 and Blake, D. R.: Boreal forest fire emissions in fresh Canadian smoke plumes: C1-C10 volatile organic compounds
879 (VOCs), CO₂, CO, NO₂, NO, HCN and CH₃CN, *Atmos. Chem. Phys.*, 11(13), 6445–6463, doi:10.5194/acp-11-6445-
880 2011, 2011.

881 Sommariva, R., De Gouw, J. A., Trainer, M., Atlas, E., Goldan, P. D., Kuster, W. C., Warneke, C. and Fehsenfeld, F. C.:
882 Emissions and photochemistry of oxygenated VOCs in urban plumes in the Northeastern United States, *Atmos. Chem.*
883 *Phys.*, 11(14), 7081–7096, doi:10.5194/acp-11-7081-2011, 2011.

884 Sommers, W. T., Loehman, R. A. and Hardy, C. C.: Wildland fire emissions, carbon, and climate: Science overview and

885 knowledge needs, *For. Ecol. Manage.*, 317, 1–8, doi:10.1016/j.foreco.2013.12.014, 2014.

886 Stockwell, C. E., Veres, P. R., Williams, J. and Yokelson, R. J.: Characterization of biomass burning emissions from
887 cooking fires, peat, crop residue, and other fuels with high-resolution proton-transfer-reaction time-of-flight mass
888 spectrometry, *Atmos. Chem. Phys.*, 15(2), 845–865, doi:10.5194/acp-15-845-2015, 2015.

889 United Nations: World Population Prospects: The 2017 Revision, Dep. Econ. Soc. Aff. - Popul. Div., 2017.

890 Wang, M., Shao, M., Chen, W., Yuan, B., Lu, S., Zhang, Q., Zeng, L. and Wang, Q.: A temporally and spatially resolved
891 validation of emission inventories by measurements of ambient volatile organic compounds in Beijing, China, *Atmos.*
892 *Chem. Phys.*, 14(12), 5871–5891, doi:10.5194/acp-14-5871-2014, 2014.

893 Wang, Y.-F., Owen, S. M., Li, Q.-J. and Peñuelas, J.: Monoterpene emissions from rubber trees (*Hevea brasiliensis*) in a
894 changing landscape and climate: chemical speciation and environmental control, *Glob. Chang. Biol.*, 13(11), 2270–2282,
895 doi:10.1111/j.1365-2486.2007.01441.x, 2007.

896 Warneke, C., McKeen, S. a., de Gouw, J. a., Goldan, P. D., Kuster, W. C., Holloway, J. S., Williams, E. J., Lerner, B. M.,
897 Parrish, D. D., Trainer, M., Fehsenfeld, F. C., Kato, S., Atlas, E. L., Baker, a. and Blake, D. R.: Determination of urban
898 volatile organic compound emission ratios and comparison with an emissions database, *J. Geophys. Res.*, 112(D10),
899 D10S47, doi:10.1029/2006JD007930, 2007.

900 Wiedinmyer, C., Yokelson, R. J. and Gullett, B. K.: Global Emissions of Trace Gases, Particulate Matter, and Hazardous
901 Air Pollutants from Open Burning of Domestic Waste, *Environ. Sci. Technol.*, 48(16), 9523–9530, doi:10.1021/es502250z,
902 2014.

903 Yokelson, R. J., Burling, I. R., Gilman, J. B., Warneke, C., Stockwell, C. E., De Gouw, J., Akagi, S. K., Urbanski, S. P.,
904 Veres, P., Roberts, J. M., Kuster, W. C., Reardon, J., Griffith, D. W. T., Johnson, T. J., Hosseini, S., Miller, J. W., Cocker,
905 D. R., Jung, H. and Weise, D. R.: Coupling field and laboratory measurements to estimate the emission factors of identified
906 and unidentified trace gases for prescribed fires, *Atmos. Chem. Phys.*, 13(1), 89–116, doi:10.5194/acp-13-89-2013, 2013.

907 Zhang, Q., Yuan, B., Shao, M., Wang, X., Lu, S., Lu, K., Wang, M., Chen, L., Chang, C.-C. and Liu, S. C.: Variations of
908 ground-level O₃ and its precursors in Beijing in summertime between 2005 and 2011, *Atmos. Chem. Phys.*, 14(12), 6089–
909 6101, doi:10.5194/acp-14-6089-2014, 2014.

910

911

912 **List of figures**

913 **Figure 1.** Geographical location of Abidjan, Côte d'Ivoire and spatial distribution of ambient VOC measurements.
914 Red stars indicate the VOC measurement sites and the blue square represents the meteorology site. More
915 information about the ambient site is detailed in Table 2.

916 **Figure 2.** Meteorological data observed in Abidjan, Côte d'Ivoire. The figure represents a) the weekly
917 accumulated precipitation (in mm month⁻¹) and weekly mean air temperature (in °C) and b) the wind speed (in m
918 s⁻¹) and direction observed (deg), during the field campaigns (2016). Data was downloaded from the National
919 Centers for environmental information site (NCDC), NOAA and recorded at Abidjan International Airport (see
920 location in Figure 1).

921 **Figure 3.** Spatial distribution of VOCs measured at ambient sites in Abidjan, size-coded by the sum of VOCs (in
922 μg m⁻³) and color-coded by the relative contribution of BTEX compounds (% in mass), namely m+p-xylene (m+p-
923 xyl), toluene (Tol), o-xylene (o-xyl), ethylbenzene (EthylB), benzene (Benz), and other VOC. Values shown in
924 each pie-chart represent the total VOC concentration measured at the sampling point. Ambient site names and
925 characteristics are presented in Table 2.

926 **Figure 4.** Boxplot showing the VOC concentrations (μg m⁻³) at Abidjan ambient sites (upper panel). The middle
927 line in each box plot indicates the median (50th percentile), the lower and upper box limits represent the 25th and
928 75th quartiles, respectively, and the whiskers the 99% coverage assuming the data has a normal distribution. The
929 lower panel shows the mean concentrations reported in other cities worldwide, such as Abidjan – Côte d'Ivoire
930 (this study), Paris- France (AIRPARIF, 2016), São Paulo - Brazil (Dominutti et al., 2016), Beirut - Lebanon
931 (Salameh et al., 2014), Karachi – Pakistan (Barletta et al., 2002) and Welgegend- South Africa (Jaars et al., 2014).

932 **Figure 5.** Relative concentration comparison between ambient measurements and emission source profiles of
933 VOCs measured in Abidjan, Côte d'Ivoire. Orange and yellow based colours represent the contributions of
934 alkanes, blue based colours aromatics, and green-based colours terpenes and isoprene.

935 **Figure 6.** Contribution of VOC reported in Table S1 to the measured molar mass of anthropogenic sources
936 analysed in Abidjan, aggregated in VOC families (Table S2). The emission sources under analysis are heavy-duty
937 diesel vehicles (HDDV), two-wheel two-stroke vehicles (TW2T), two-wheel four-stroke vehicles (TW4T), light-
938 duty diesel vehicles (LDDV), light-duty gasoline vehicles (LDGV), charcoal burning (CH), wood fuel burning
939 (FW), charcoal making (CHM) and landfill waste burning (WB). Values in the upper panel represent the total
940 measured molar mass (in μg cm⁻³ ppm CO⁻¹) of the respective anthropogenic source.

941 **Figure 7.** Contributions of VOC emission ratios to (a)–(d) the measured molar mass, (e)–(h) OH reactivity, (i)–
942 (l) relative ozone formation potential POCP and (m)–(p) relative SOA formation potential, aggregated in VOC
943 families. Absolute totals for each source are shown below each pie chart in the respective units.

944 **Figure 8.** Comparison of VOC emission profiles for Côte d'Ivoire from the emissions estimated from the
945 measurements of this study and the EDGAR v4.3.2 (Huang et al., 2017) and MACCity inventories (Granier et al.,
946 2011). The profile analysis integrates road transportation and residential sectors based on the sector activity for
947 2012. a) absolute emissions, in Tg year⁻¹, b) relative mass contribution, and c) relative mass reactivity, considering
948 100 Tg of emissions weighted by the k_{OH} reaction rate calculated for each VOC family.

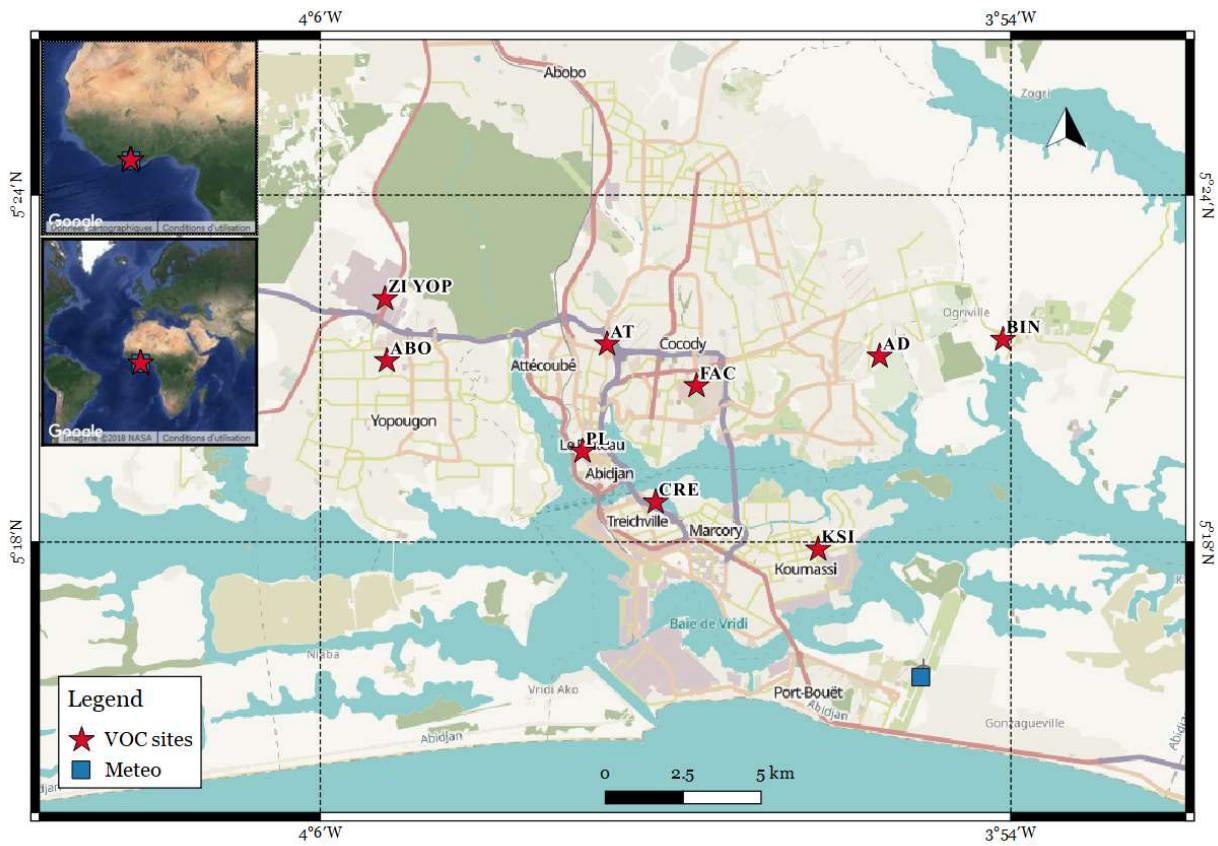
949 **Figure 9.** VOC emission profiles considering all the VOC families calculated from the measurements of our study
950 and compared with the global EDGAR v4.3.2 inventory (Huang et al., 2017). The comparison integrates road
951 transportation (RT) and residential (Resid) sectors in Côte d'Ivoire and Europe for the year 2012. Absolute
952 emissions are expressed in Gg year⁻¹ for each VOC group.

953 **Figure 10.** Total estimated emissions and relative distributions in the anthropogenic sources measured in Côte
954 d'Ivoire for the VOC family a) Terpenes, b) IVOCs and c) Aldehydes (* for aldehydes species >C₆).

955 **Figure 11.** Distribution of monoterpenes and isoprene in the emission sources measured in Abidjan. The values
956 represent the percentage of each terpenoids over the total emission estimated for these species.

957

958

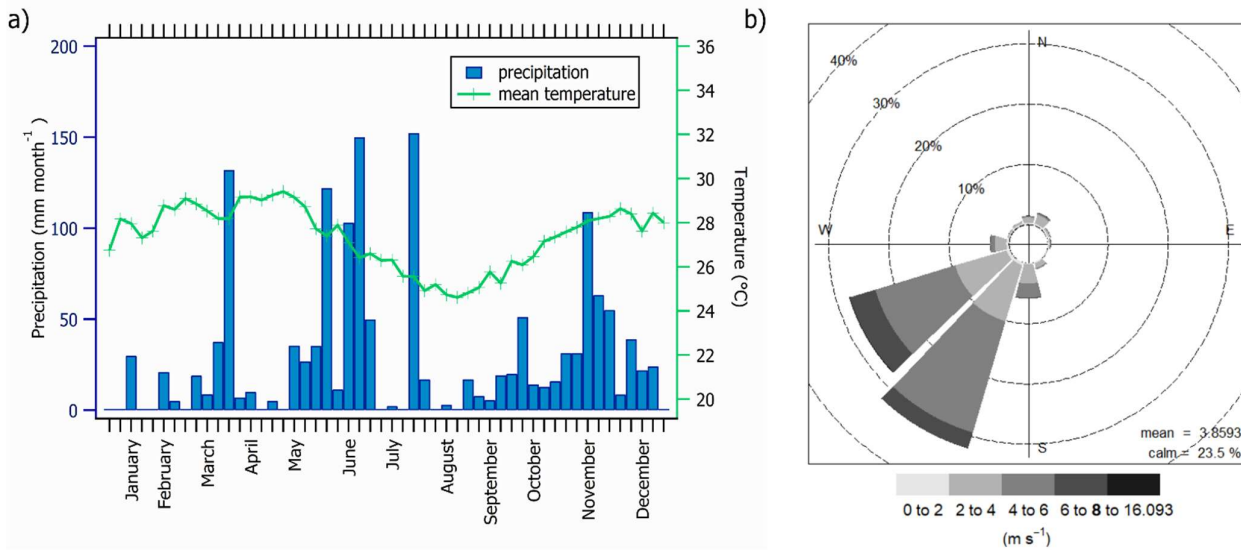


959

960 **Figure 1.** Geographical location of Abidjan, Côte d'Ivoire and spatial distribution of ambient VOC measurements.

961 Red stars indicate the VOC measurement sites and the blue square represents the meteorology site. More
 962 information about the ambient site is detailed in Table 2.

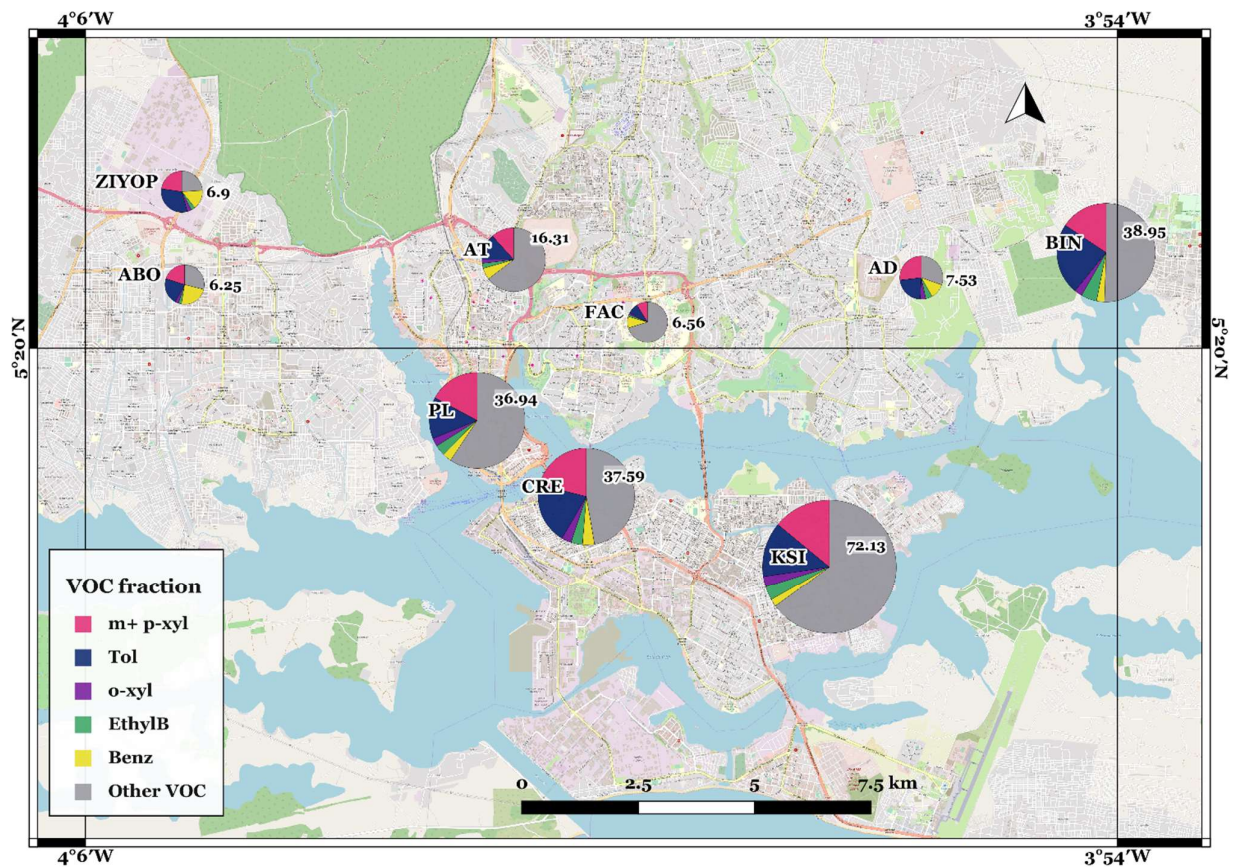
963



964

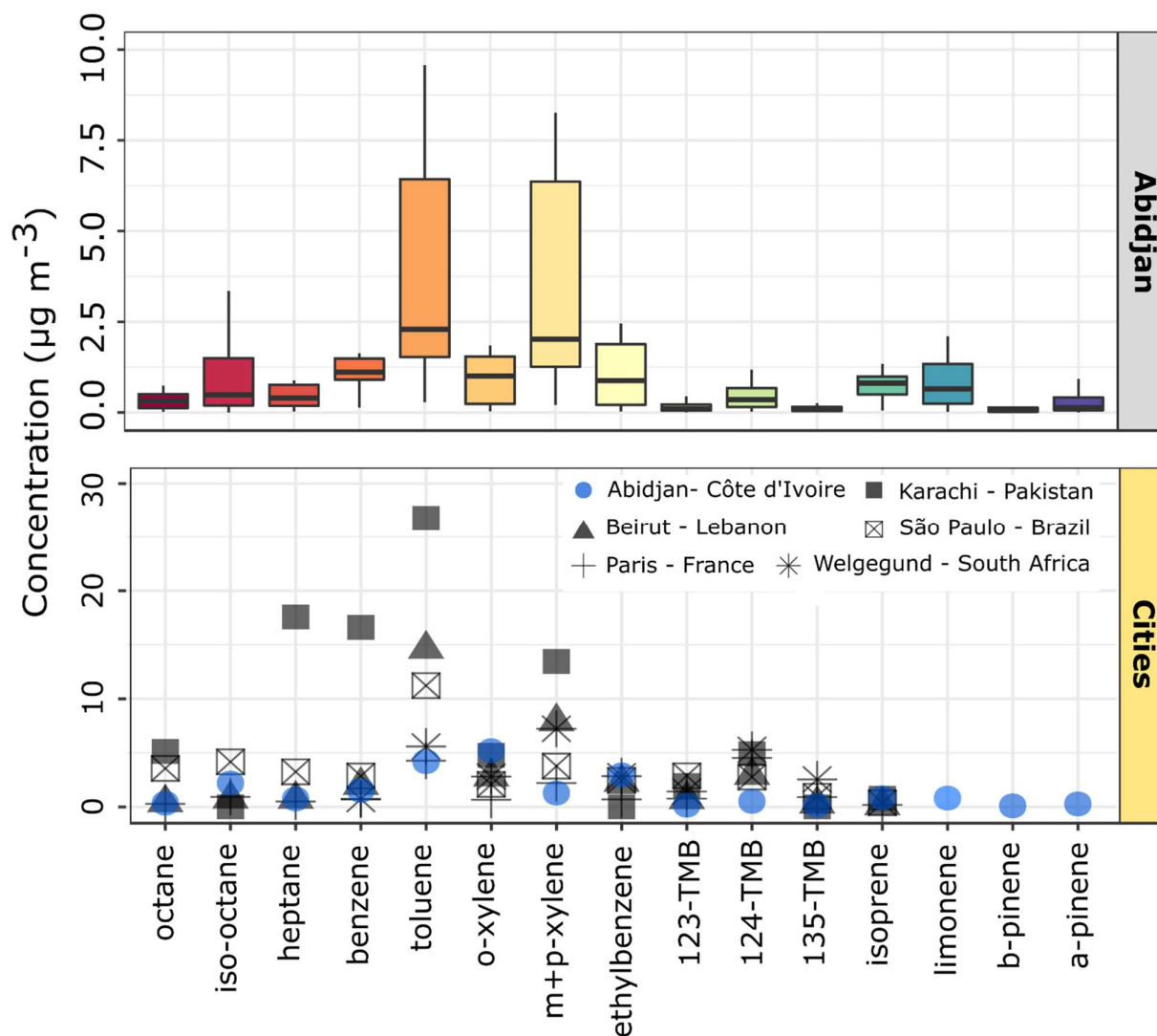
965 **Figure 2.** Meteorological data observed in Abidjan, Côte d'Ivoire. The figure represents a) the weekly
 966 accumulated precipitation (in mm month⁻¹) and weekly mean air temperature (in °C) and b) the wind speed (in m
 967 s⁻¹) and direction observed (deg), during the field campaigns (2016). Data was downloaded from the National
 968 Centers for environmental information site (NCDC), NOAA and recorded at Abidjan International Airport (see
 969 location in Figure 1).

970



971
 972 **Figure 3.** Spatial distribution of VOCs measured at ambient sites in Abidjan, size-coded by the sum of VOCs (in
 973 $\mu\text{g m}^{-3}$) and color-coded by the relative contribution of BTEX compounds (% in mass), namely m+p-xylene (m+p-
 974 xyl), toluene (Tol), o-xylene (o-xyl), ethylbenzene (EthylB), benzene (Benz), and other VOC. Values shown in
 975 each pie-chart represent the total VOC concentration measured at the sampling point. Ambient site names and
 976 characteristics are presented in Table 2.

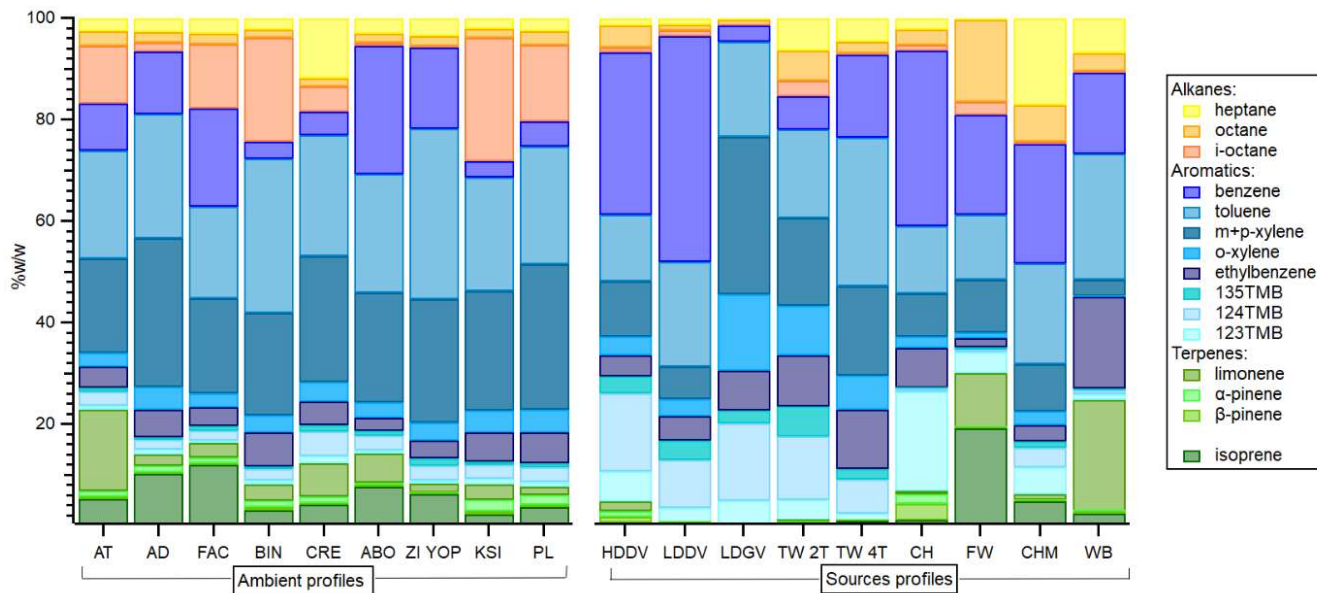
977



978
979

980 **Figure 4.** Boxplot showing the VOC concentrations ($\mu\text{g m}^{-3}$) at Abidjan ambient sites (upper panel). The middle
981 line in each box plot indicates the median (50th percentile), the lower and upper box limits represent the 25th and
982 75th quartiles, respectively, and the whiskers the 99% coverage assuming the data has a normal distribution. The
983 lower panel shows the mean concentrations reported in other cities worldwide, such as Abidjan - Côte d'Ivoire
984 (this study), Paris - France (AIRPARIF, 2016), São Paulo - Brazil (Dominutti et al., 2016), Beirut - Lebanon
985 (Salameh et al., 2014), Karachi - Pakistan (Barletta et al., 2002) and Welgegund - South Africa (Jaars et al., 2014).

986



988

989 **Figure 5.** Relative concentration comparison between ambient measurements and emission source profiles of
 990 VOCs measured in Abidjan, Côte d'Ivoire. Orange and yellow based colours represent the contributions of
 991 alkanes, blue based colours aromatics, and green-based colours terpenes and isoprene.

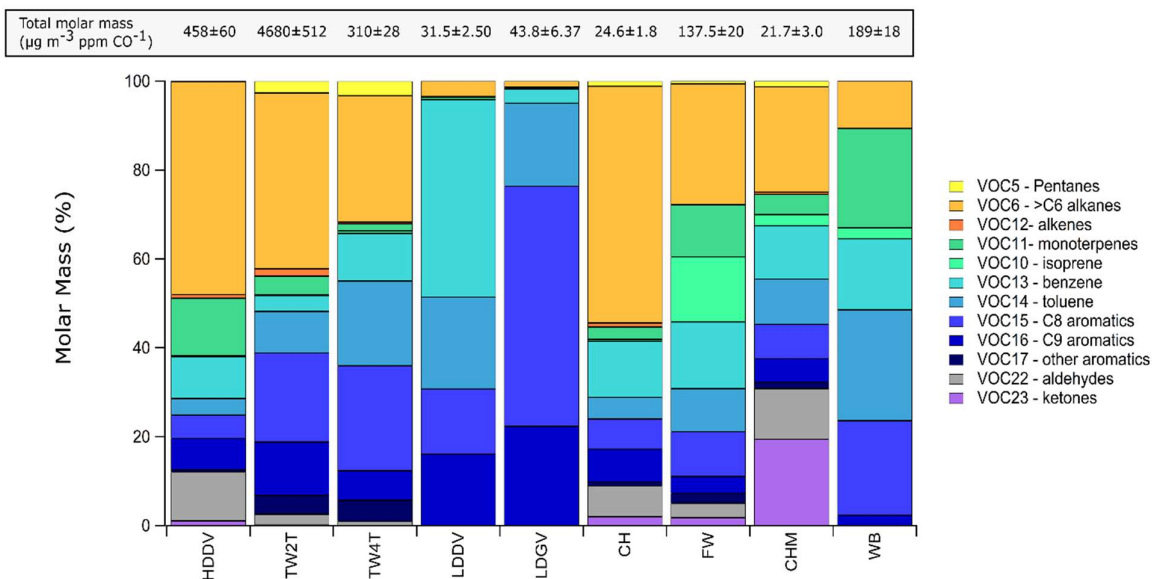
992

993

994

995

996



997

998 **Figure 6.** Contribution of VOC reported in Table S1 to the measured molar mass of anthropogenic sources

999 analysed in Abidjan, aggregated in VOC families (Table S2). The emission sources under analysis are heavy-duty

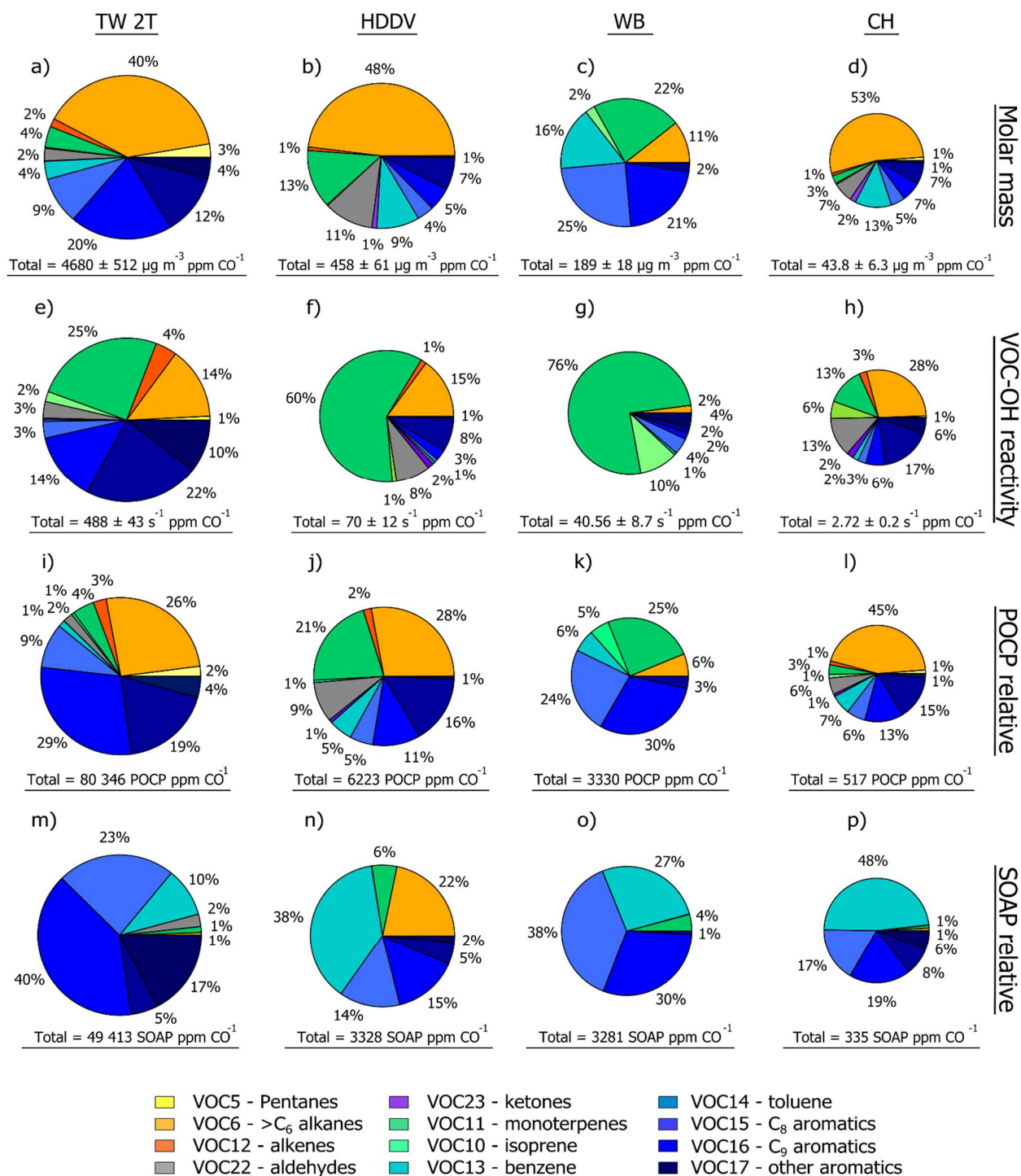
1000 diesel vehicles (HDDV), two-wheel two-stroke vehicles (TW2T), two-wheel four-stroke vehicles (TW4T), light-

1001 duty diesel vehicles (LDDV), light-duty gasoline vehicles (LDGV), charcoal burning (CH), wood fuel burning

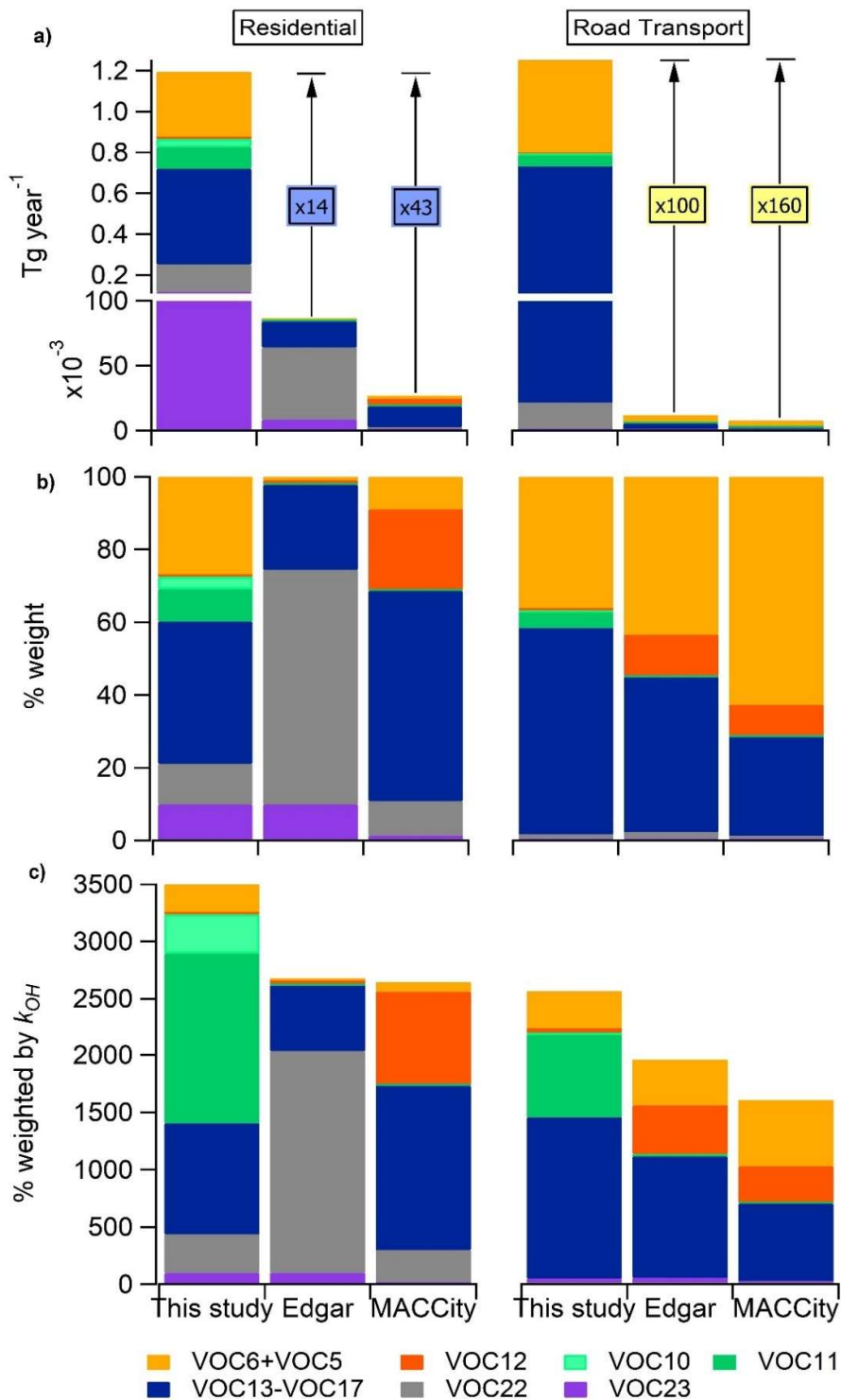
1002 (FW), charcoal making (CHM) and landfill waste burning (WB). Values in the upper panel represent the total

1003 measured molar mass (in $\mu\text{g cm}^{-3}$ ppm CO^{-1}) of the respective anthropogenic source.

1004

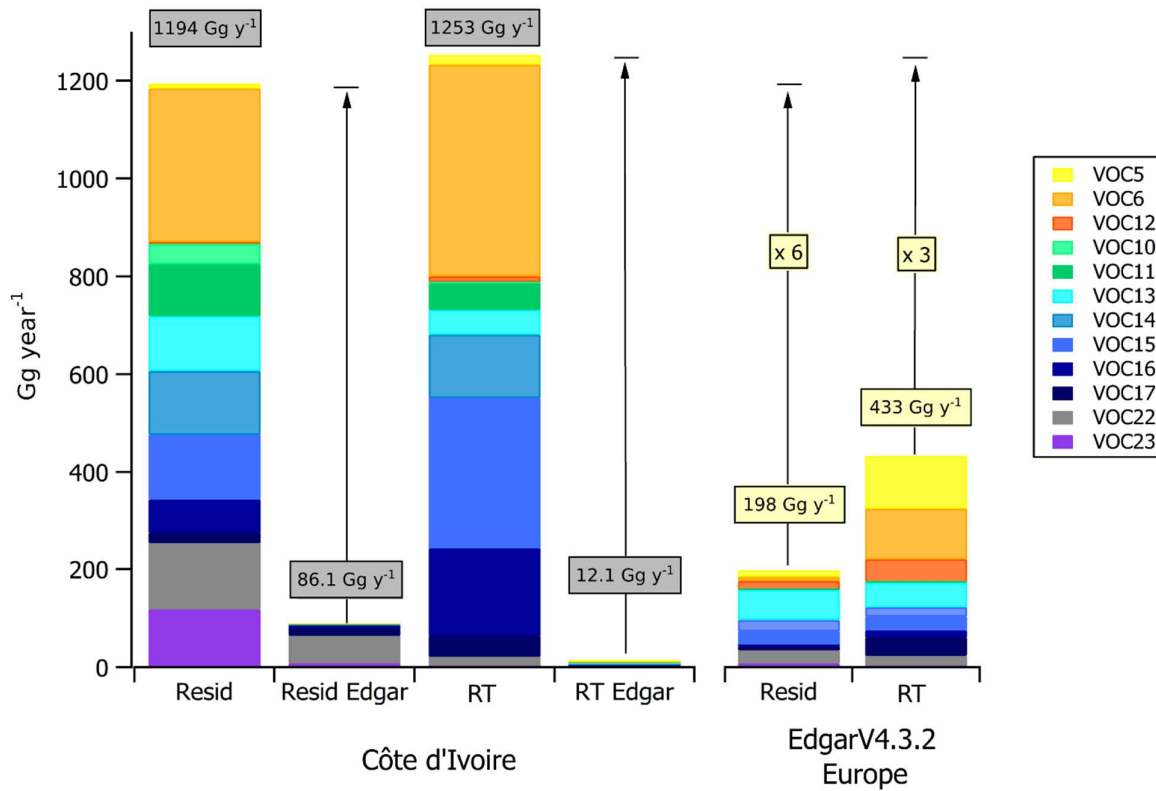


1009 **Figure 7.** Contributions of VOC emission ratios to (a)–(d) the measured molar mass, (e)–(h) OH reactivity, (i)–
 1010 (l) relative ozone formation potential POCP and (m)–(p) relative SOA formation potential, aggregated in VOC
 1011 families. Absolute totals for each source are shown below each pie chart in the respective units.



1014

1015 **Figure 8.** Comparison of VOC emission profiles for Côte d'Ivoire from the emissions estimated from the
 1016 measurements of this study and the EDGAR v4.3.2 (Huang et al., 2017) and MACCity inventories (Granier et al.,
 1017 2011). The profile analysis integrates road transportation and residential sectors based on the sector activity for
 1018 2012. a) absolute emissions, in Tg year^{-1} , b) relative mass contribution, and c) relative mass reactivity, considering
 1019 100 Tg of emissions weighted by the k_{OH} reaction rate calculated for each VOC family.



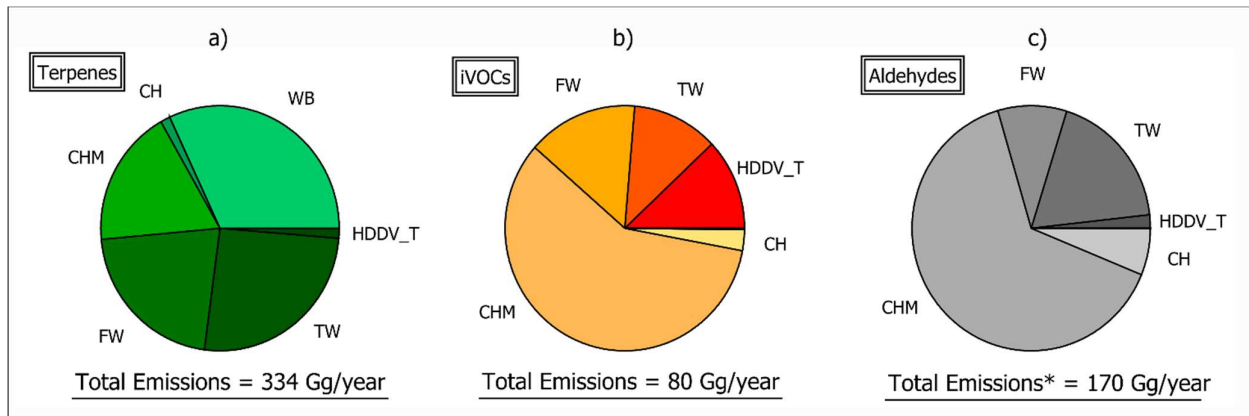
1021

1022 **Figure 9.** VOC emission profiles considering all the VOC families calculated from the measurements of our study
 1023 and compared with the global EDGAR v4.3.2 inventory (Huang et al., 2017). The comparison integrates road
 1024 transportation (RT) and residential (Resid) sectors in Côte d'Ivoire and Europe for the year 2012. Absolute
 1025 emissions are expressed in Gg year⁻¹ for each VOC group.

1026

1027

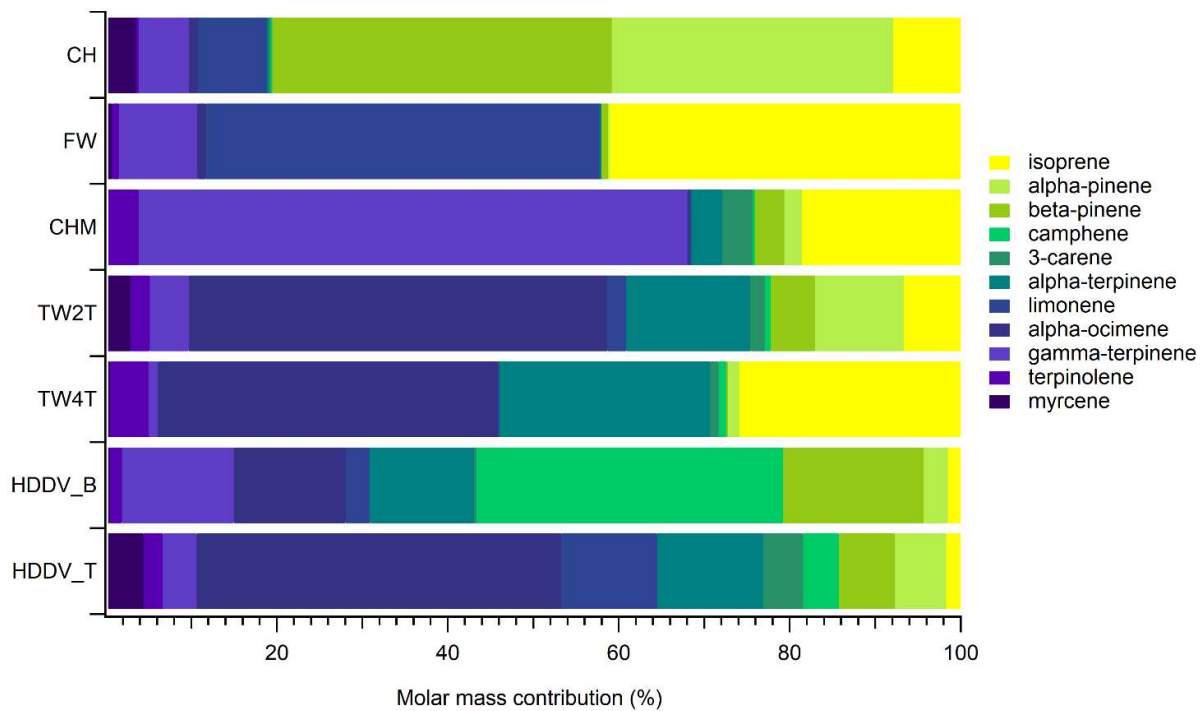
1028



1029

1030 **Figure 10.** Total estimated emissions and relative distributions in the anthropogenic sources measured in Côte
1031 d'Ivoire for the VOC family a) Terpenes, b) iVOCs and c) Aldehydes (* for aldehydes species >C₆).

1032



1033

1034 **Figure 11.** Distribution of monoterpenes and isoprene in the emission sources measured in Abidjan. The values
 1035 represent the percentage of each terpenoids over the total emission estimated for these species.

1036

1037

1038

1039

1040 **List of Tables**

1041

1042 Table 1. Description of the emission sources measured and evaluated in Abidjan, Côte d'Ivoire.

1043 Table 2. Geographical location and characteristics of ambient measurement sites in Abidjan, Côte d'Ivoire

1044

1045

Table 1. Description of the emission sources measured and evaluated in Abidjan, Côte d'Ivoire.

Reference	Sub-group	Description	source	type
HDDV		Heavy-duty diesel vehicles	Diesel emissions	Road Transport
	HDDV-T	Diesel trucks	Diesel emissions	Road Transport
	HDDV-B	Diesel buses	Diesel emissions	Road Transport
LDDV		Light-duty diesel vehicles	Diesel emissions	Road Transport
LDGV		Light-duty gasoline vehicles	Gasoline emissions	Road Transport
TW	TW2T	Two-wheel two-stroke	a mixture of smuggled oil and gasoline	Road Transport
	TW4T	Two-wheel four-stroke	a mixture of smuggled oil and gasoline	Road Transport
CH		Charcoal	Charcoal burning	Residential
FW		Fuelwood burning	<i>Hevea brasiliensis</i>	Residential
CHM		Charcoal making	Charcoal fabrication	Residential
WB		Waste burning	Domestic landfill burning	Waste burning

1050

1051

1052

Table 2. Geographical location and characteristics of ambient measurement sites in Abidjan, Côte d'Ivoire

ID	Site location	Longitude	Latitude	Activity
AT	Adjame	04°01'04"W	05°21'14"N	Traffic site. Site near a gbaka public transport station; regular traffic jams; obsolete public transport vehicles (gbaka, shared taxis and buses); human activities
AD	Akouédo	03°56'16"W	05°21'12"N	Landfill waste burning Uncontrolled landfill, continuous waste burning of all types of waste
FAC	Cocody	03°59'27"W	05°20'42"N	Residential. University residences; electric vehicles; new personal vehicles; use of liquefied petroleum gas (LPG) for cooking
BIN	Bingerville	03°54'07"W	05°21'30"N	Urban Background Far from traffic, near to Ebrié Lagoon
CRE	Treichville	04°00'10"W	05°18'41"N	Green urban area, Near to Ebrié Lagoon; windy
ABO	Abobo	04°04'10"W	05°26'08"N	Traffic + residential Townhall, near to the big market of Abobo. Old communal taxis and minibuses in a crowded crossroad, human activities
ZI YOP	Yopougon	04°04'52"W	05°22'12"N	Industrial area Heavy industries (cement plants) and light industries (agro-industries, plastic and iron processing, pharmaceutical and cosmetics industries); heavy goods vehicles, traffic jams
KSI	Koumassi	03°57'20"W	05°17'52"N	Domestic fires + traffic Residential site mainly influenced by domestic activities, fire-wood, and charcoal; old vehicles.
PL	Plateau	04°01'26"W	05°19'33"N	Traffic/administrative City center, crossroad with traffic jams; light-duty vehicles, near the train station

1053

1054